Main revisions and response to reviewers' comments

Manuscript No.: acp-2018-984

Title: Top-down estimate of black carbon emissions for city cluster using ground observations: A case study in southern Jiangsu, China

Authors: Xuefen Zhao, Yu Zhao, Dong Chen, Chunyan Li, Jie Zhang

We thank very much for the valuable comments and suggestions from the three reviewers, which help us improve our manuscript significantly. The comments were carefully considered and revisions have been made in response to suggestions. Following is our point-by-point responses to the comments and corresponding revisions.

Reviewer #1

0. *The authors provide a detailed analysis to constrain BC emissions from Jiangsu (China) using observations from two stations. They found BC emissions are significantly overestimated in the bottom-up inventories, which has important implications. However, I have some major concerns about the representation of their stations to the whole region, and the inversion methodology. I recommend the paper for publication after consideration of the points below.*

Response and revisions:

We appreciate the reviewer's remarks on the importance of the work. Regarding the limitations pointed out by the reviewer, we have improved the manuscript accordingly. The spatial representativeness of the two sites in the multiple regression model has been clearly described (please see our response to Q3). Case 2 in which observation data at only one site (NJU) were used has been further re-analysed to avoid confusion to the inversion methodology (please see our response to Q4).

1. *Abstract Lines 28-29, please confirm the same BC concentrations (i.e. 3.4 ug/m^3) at both sites. In addition, Lines 39-40 say: "the simulated annual mean was elevated to 2.6". I assume it is elevated from 3.4 to 2.6?*

Response and revisions:

We thank the reviewer's comment and reminder. We confirmed that the annual mean simulations of BC were 3.44 and 3.39 ug/m^3 at NJU and PAES, respectively. When the constrained emissions were applied, the annual mean concentration was simulated to decrease from 3.39 to 2.57 ug/m^3 at PAES, and it was indicated **in Table 2 in the revised manuscript**. We corrected the sentence **in line 41 in the revised manuscript**: "At PAES, in particular, the simulated annual mean declined to 2.6 μg/m^3 and the annual normalized mean error (NME) decreased from 72.0% to 57.6%."

2. *Line 257-258 Are 5 days long enough to minimize the influences of initial conditions? I checked the methodology of other studies and found much longer initialization periods. For example, 3 months in Wang et al. (2013) and Mao et al. (2015).*

Response and revisions:

We thank and agree with the reviewer's comment. Some studies that applied GEOS-Chem or WRF-Chem to constrain BC emissions at larger spatial scale often chose several months as spin up to minimize the influence of initial conditions (Fu et al., 2013 and studies mentioned by the reviewer). For WRF-CMAQ model, in contrast, more studies used several days as initialization periods, for example, 5 days in Chang et al. (2018) and Tran et al. (2018), and 7 days in Ran et al. (2016). The period in this study is expected to be sufficient to minimize the influence of initial condition.

3. *Table 2 As shown with the annual mean result:*

** NJU, the a priori is 0.4 lower than obs, and is reduced by 0.6 in the inversion. The a posteriori is 1.0 lower than obs.*

** PAES, the a priori is 0.9 higher than obs, and is reduced by 0.8 in the inversion. The a posteriori is 0.1 higher than obs.*

It seems that the inversion simply moves the bias from PAES to NJU by reducing the total emissions, suggesting the inversion system is dominated by PAES. Considering the inconsistency between NJU and PAES, it is hard to say whether the conclusion is reliable to provide a good representation for the whole region.

Response and revisions:

We appreciate the reviewer's important comment. As can been seen **in Table 2 and Figures 3 and 4 in the revised manuscript**, application of JS-posterior effectively reduced the large biases between simulations and observations for all seasons at PAES and for January and April at NJU, suggested by the reduced NMEs. In particular, most of the overestimations in peak concentrations were corrected at the both sites. We mentioned **in lines 489-492, 497-499 and 508 in the revised manuscript**. It should be also acknowledged that NMEs for July and October and the annual average of NME were slightly enhanced at NJU. Limitation of the multiple regression model was thus indicated that overestimation and underestimation in concentrations at different sites could hardly be corrected simultaneously without further improvement in spatial distribution of emissions, and we mentioned in details **in lines 511-516 in the revised manuscript**.

To improve the method and to quantify the effect of spatial representation of observation sites on top-down estimate, we provided Case 3 in which observation data at PAES and NJU were applied to constrain emissions from Nanjing and Suzhou-Wuxi-Changzhou-Zhenjiang city cluster, respectively, **in Section 4.1 in the revised manuscript**. The best CTM performance was obtained in Case 3, implying that inclusion of more measurement data with their spatial representativeness considered could improve the top-down method. Given the limited BC observation data in the area, therefore, more measurements with better spatiotemporal coverage were recommended for constraining BC emissions effectively, as mentioned **in lines 47-52 in the revised manuscript**.

4. *Section 4.1 As shown in Table 2, the model simulation (2.38) is already lower than obs (2.69) in April at NJU. When only NJU data is used, how could the inversion keep reducing the emissions with scaling factors, 0.42, 0.95 and 0.65? Theoretically, an inversion system should minimize the discrepancy between model and obs rather than magnifying it.*

Response and revisions:

We thank the reviewer's important comment. As can been seen **in Table 2 in the revised manuscript**, the monthly mean of simulated BC concentrations at NJU with JS-prior was 2.38 ug/m^3 for all periods in April, smaller than the observed 2.69 ug/m^3. For Case 2 in which only NJU data were applied, the scaling factors for industry, residential and transportation emissions were obtained at 0.42, 0.95, and 0.65, respectively, implying a further reduction in BC emissions. The main reason is that the data for the whole April were not fully used due to necessary data screening in the multiple regression model. We acknowledge that the data screening process was not clearly stated in the original manuscript. Before applying in the multiple regression model, we excluded the periods following the criterions: the periods lack of observation data, those for which the contribution of each emission sector (power generation, industry, residential sources and transportation) was simulated to be smaller than zero through the brute-force method, and those for which the sum of contributions of all the four sectors was larger than 100% with CTM. The data screening helped to reduce the uncertainty of CTM in the multiple regression model. We added the description of data screening **in lines 240-245 in the revised**

manuscript. The number of data after screening in Case 2 was 48% of data in all periods (most data screening was due to lack of observations, accounting for 38%). We divided all the data points in April in Case 2 into two groups: those included in the multiple regression model and those excluded from the model, and analyzed the modeling performances for both groups separately. As can be seen in Table R1, the simulated concentration for periods included in the multiple regression model (2.71 μg/m^3) was larger than the observation (2.56 μg/m^3) when JS-prior was applied, different from the case without data screening (i.e., data in all periods were included). The emissions could then be reduced when the observation was applied in the constraining. As a result, application of the top-down estimate in Case 2 effectively reduced the NME for the period included in the model from 34.01% to 21.09%, and the simulated average concentration was closer to the observation. At the same time, the constrained emissions did not increase the bias for periods excluded from the multiple regression model. It thus indicated that the underestimation for periods excluded from the multiple regression model could result largely from factors other than emissions like meteorology. We added the analysis **in lines 547-559 in the revised manuscript** and included Table R1 **as Table S8 in the revised supplement**.

Table R1. Statistical indicators for observed and simulated BC concentrations for all periods, those included in the multiple regression model, and those excluded from the model in JS-prior and Case 2 for April 2015 at NJU.

Site	Parameter	JS-prior: All period	JS-prior: Included	JS-prior: Excluded	Case 2: All period	Case 2: Included	Case 2: Excluded
NJU	Average SIM (μg/m^3)	2.38	2.71	2.08	2.27	2.42	2.08
	Average OBS (μg/m^3)	2.69	2.56	2.99	2.69	2.56	2.99
	NMB (%)	-16.02	5.90	-56.48	-21.59	-5.32	-56.63
	NME (%)	42.31	34.01	57.62	32.47	21.09	57.61

5. *Table 4 More information is needed in the caption. It is really difficult to follow the discussion to distinguish the Cases (B, 1, 2, 3, 4, 5) and Cases (6, 7).*

Response and revisions:

We thank the reviewer's reminder. As suggested by the reviewer, we added the introduction of different cases **in Table 3 in the revised manuscript**.

References

Fu, T. M., Cao, J. J., Zhang, X. Y., Lee, S. C., Zhang, Q., Han, Y. M., Qu, W. J., Han, Z., Zhang, R., Wang, Y. X., Chen, D., and Henze, D. K.: Carbonaceous aerosols in China: top-down constraints on primary sources and estimation of secondary contribution, Atmospheric Chemistry and Physics, 12, 2725-2746, 10.5194/acp-12-2725-2012, 2012.

Chang, X., Wang, S., Zhao, B., Cai, S., and Hao, J.: Assessment of inter-city transport of particulate matter in the Beijing-Tianjin-Hebei region, Atmospheric Chemistry and Physics, 18, 4843-4858, 10.5194/acp-18-4843-2018, 2018.

Trang, T., Huy, T., Mansfield, M., Lyman, S., and Crosman, E.: Four dimensional data assimilation (FDDA) impacts on WRF performance in simulating inversion layer structure and distributions of CMAQ-simulated winter ozone concentrations in Uintah Basin, Atmospheric Environment, 177, 75-92, 10.1016/j.atmosenv.2018.01.012, 2018.

Ran, L., Pleim, J., Gilliam, R., Binkowski, F. S., Hogrefe, C., and Band, L.: Improved meteorology from an updated WRF/CMAQ modeling system with MODIS vegetation and albedo, Journal of Geophysical Research-Atmospheres, 121, 2393-2415, 10.1002/2015jd024406, 2016.

Reviewer #2

0. *In this study, Zhao et al. uses ground-based elemental carbon (EC) measurements from two sites in eastern China to evaluate and constrain black carbon (BC) emissions from two bottom-up inventories: a national/regional inventory for China (MEIC) and a high-resolution inventory for city clusters in southern Jiangsu Province. Both inventories include emissions from transportation, industry, power generation, and the residential sector. The authors show that the posterior emission estimates, constrained by ground measurements, are much smaller than the prior emission estimates, suggesting that pollution control measures by the Jiangsu government have effectively reduced emissions of BC. They also show results from various sensitivity tests, including those on the number of observation sites, spatial representativeness of observation sites, a priori emission inventories, and wet deposition. Overall, this is an interesting study that can be potentially useful for air quality modeling and management, emission inventory development and evaluation, and also studies on regional aerosol effects. Through several fairly detailed sensitivity tests, the authors also demonstrate that the differences between a priori and posteriori emission estimates are robust. However, the paper is overly long (and needs some improvement in presentation quality) and some reorganization may help. And there are also some concerns about the methodology that need to be addressed before this paper can be published in ACP.*

Response and revisions:

We appreciate the reviewer's remarks on the importance of the work. We reorganized Figures and Tables following the reviewer's suggestions (please see our response to Q3 and Q7) and specified the methodology of top-down estimate (please see our response to Q1-2). Please see the details in the following response and revision list to the reviewer's comment.

1. *Major comments: It is not quite clear whether emissions outside of Jiangsu Province (but within the model domains) are scaled or not. Given the location of the sites, they could be strongly influenced by emissions from nearby provinces. If different local governments implemented different pollution control measures but the same domain wide scaling factors are used for emissions, that may lead to biases in the final estimated emissions for southern Jiangsu.*

Response and revisions:

We appreciate the reviewer's important comment. For MEIC-prior and JS-prior, emissions from different provinces and cities within the modeling domain were scaled based mainly on changes in their respective activity levels from 2012 to 2015, including those outside of Jiangsu Province. However, we did not constrain the emissions outside of Jiangsu Province in the top-down method, and we agree the limitation here. The main reason is that there were very few BC observation data available in the cities outside southern Jiangsu. Using observations at NJU or PAES to constrain emissions from those cities would bring more uncertainty for the cases in which local emissions dominated the air quality. Given this limitation, therefore, more measurements with better spatial coverage were recommended to be conducted and published for constraining BC emissions effectively in the future. We discussed this **in lines 545-547 in the revised manuscript**.

The uncertainty of using observations at two sites to constrain emissions from southern Jiangsu was expected to be insignificant in this work. Located in the downwind of the Yangtze River Delta region (YRD), NJU is more representative for the emissions from western YRD through regional transport. PAES is in urban Nanjing and its air quality is commonly influenced by surrounding transportation and residential sources, thus PAES is representative for the local emissions of Nanjing. We quantified the contribution of Nanjing and Suzhou-Wuxi-Changzhou-Zhenjiang city cluster through the brute-force method **in Sector 4.1 in the revised manuscript**. As can be seen **in Figure S10 in the revised supplement**, the monthly mean contributions of the emissions from the two regions in April were aggregated at 54%

and 59% at NJU and PAES respectively. We thus believe it is reasonable to use observations at two sites to constrain emissions from southern Jiangsu.

Regarding the influence of emissions outside southern Jiangsu, the contribution of each sector (c_{power}, $c_{industry}$, $c_{residential}$, and $c_{transportation}$) **in Eq1 in the revised manuscript** was simulated when the emissions from that sector were zeroed out for the whole third domain. It means that the emissions outside southern Jiangsu were also considered in the multiple regression model to obtain scaling factors. We applied the scaling factors to constrain emissions from southern Jiangsu only while remaining emissions outside southern Jiangsu unchanged so that it could better quantify the improvement of modeling performance at two sites due to the top-down estimate in southern Jiangsu. We acknowledge the uncertainty of including emissions of the whole third domain in the multiple regression model, due to different implementation of pollution control measures by city. As shown in Table R2, we compared the reduction rates of monthly BC emissions in the national inventory MEIC from 2012 to 2015 inside and outside southern Jiangsu in the domain. The difference between the two regions was less than 6%, implying the similar progress of pollution control measurements in two regions. Due to limited BC observations, moreover, we also checked the annual reduction rates in $PM_{2.5}$ concentrations from 2013 to 2015 for cities in the third domain based on the observation data from China National Environmental Monitoring Center (http://www.cnemc.cn/). As shown in Table R3, the annual reduction rates were ranged from 10% to 17% by city, reflecting again the similar implementation of air pollution control policies around the regions. Relative statement was added **in lines 222-235 in the revised manuscript**, and Tables R2 and R3 were included as **Tables S2 and S3 in the revised supplement**.

Table R2. Reduction rates in monthly emissions from 2012 to 2015 in MEIC for southern Jiangsu and other regions within the third modeling domain.

Region	Jan.	Apr.	Jul.	Oct.
Southern Jiangsu (%)	18	18	26	21
Outside southern Jiangsu (%)	12	16	21	15

Table R3. Reduction rates in annual $PM_{2.5}$ concentration for cities within the third modeling domain from 2013 to 2015.

Province	City	Reduction rate (%)
Anhui	Hefei	15.26
Jiangsu	Nantong	15.90
	Taizhou	11.76
	Yangzhou	16.84
	Nanjing	15.58
	Suzhou	12.76
	Wuxi	10.45
	Changzhou	12.31
	Zhenjiang	12.80
Shanghai	Shanghai	10.88

2. *The lack of biomass burning emissions can be concerning. Could the model underestimates of BC in July and particularly October be caused by the biomass burning (particularly agricultural fires)? How does the lack of biomass burning emissions affect the estimated emissions for other sectors?*

Response and revisions:

We thank the reviewer's comment. In both inventories (MEIC and JS), the emissions came from four sectors, including power generation, industry, residential sources and transportation, and the residential sources included fossil fuel and biofuel combustion. However, we did not include emissions from biomass open burning. In another paper of our group (Yang and Zhao, 2019), the emissions from biomass open burning in YRD were thoroughly evaluated with various methods, and the emissions were estimated to decrease by 60% from 2012 to 2015 in southern Jiangsu attributed mainly to the enhanced control of crop burning activities by the local government. With the optimized constrained method, the BC emissions from crop open burning were calculated at 0.83 Gg in southern Jiangsu 2015, contributing small in the JS-prior and JS-posterior at 3% and 6%, respectively. As shown in Table R4, in addition, the most intensive crop burning was found in May and August, indicated by the monthly fire points from satellite dectection. Limited effect of biomass burning was thus expected for the modeling periods in this study.

Table R4. Monthly fire points in southern Jiangsu for 2015, taken from Moderate Resolution Imaging Spectroradiometer (MODIS) Global Monthly Fire Location Product (MCD14ML).

2015	Jan.	Feb.	Mar.	Apr.	May	Jun.	Jul.	Aug.	Sep.	Oct.	Nov.	Dec.
Fire point	9	11	12	58	249	30	96	127	16	9	1	10

In this work, the scaling factor of residential sources in October was estimated at 1.52 in JS-posterior, implying the enhancement in BC emissions in autumn to JS-prior. The result thus implied that there were missing sources likely associated with crop waste burning in autumn, and it was discussed **in lines 420-424 in the revised manuscript**. We also evaluated the sensitivity of the constraining method to the initial emission input **in Section 4.2 in the revised manuscript**, and found the uncertainty from the a priori inventory had limited effects on the top-down estimate. To summarize, therefore, we believe that lack of biomass burning emissions in the initial inventories would not significantly bias the top-down estimation.

3. *The paper is overly long and can be better organized. In particular, if spatial representativeness and wet deposition are important, can the authors focus on the top-down estimates that consider both of these factors? Description of the other sensitivity tests can be brief. Also writing needs to be improved.*

Response and revisions:

We thank the reviewer's comment. To make the manuscript concise, we moved Figures 9 and 10 in the original manuscript to the revised supplement (Figures S11 and S12) given that the near-linearity was also indicated in previous studies (Wang et al., 2013). We integrated the original Table 8 into Table 3 in the revised manuscript to summarize the modeling performances of different cases. The scaling factors and statistical indicators in Case 7 in the original Table 9 were integrated into Table 5, while emissions by sector in Case 7 and the relative deviations compared to JS-posterior in Table 9 were integrated into Table 6. We moved the original Figure 3 that presents the seasonal variations in emissions of JS-prior, JS-posterior and MEIC-prior to the revised supplement (the new Figure S8) given the less statistical significant in seasonal patterns of several sectors in JS-posterior. We also moved the original Table 5 that summarizes the emissions from Nanjing and other cities in southern Jiangsu in different cases to Table S9 in the revised supplement. Sections 4.1 and 4.2 in the original manuscript were merged into one section (Section 4.1 in the revised manuscript) to evaluate the effects of number and spatial representativeness of observation sites on the top-down estimate. We believe the analysis on the uncertainty of the a priori inventory was important, as it could help judge the robustness of the constraining method. We found the influence of the a priori emissions was limited, and implied that the method could be potentially applied even if uncertainty existed in the bottom-up inventory. Therefore, we kept this part in the revised manuscript.

4. *Specific comments: Figure 3 and the paragraph starting from line 389: given that the scaling factor for April and Oct. are more uncertain (in terms of their statistical significance), are the seasonal patterns in the posterior emission estimates significant?*

Response and revisions:

We thank and agree with the reviewer's comment. Though the multiple regression model was statistically significant as a whole indicated by 0.00 of the overall significance in four months, the estimates for certain sources including industry in April and October and residential in April and July were more uncertain to some extent, as illustrated **in Table 1 in the revised manuscript**. It implied that the constrained emissions for those months/sources need to be cautiously applied in CTM and the seasonal patterns in those sectors could be less significant. Relevant discussion was **in lines 383-386 in the revised manuscript** and we moved original Figure 3 that presents the seasonal variations in emissions of JS-prior, JS-posterior and MEIC-prior to **Figure S8 in the revised supplement**.

5. *Figure 5a – what may have caused the model overestimates in mid-January at PAES? How does this period affect emission estimates? Can the authors exclude this period and compare the top-down estimates?*

Response and revisions:

We thank the reviewer's comment. The overestimation in January at PAES (especially in middle and late January, 16th–26th) may result from the emission control policy implemented for the National Memorial Day of Nanjing Massacre Victims in December 13th in 2014. During the period, Nanjing was undertaking series of stringent restrictions on air pollutant emissions. For example, key petrochemical and steel industries were shut down, and all the high-pollution vehicles were forbidden to drive in Nanjing. Those restrictions had large impacts on emissions and thereby air quality in the following month at PAES, but have not been fully considered in current emission inventories. Beside the emission control measures implemented in Nanjing, we evaluated the effect of planetary boundary layer (PBL) height on the modeling performance at PAES, as illustrated in Figure R1. Higher daily average PBL height was found for periods when the simulated concentrations were relatively lower (e.g., 6th -7th, 12th-15th and 28th-31st), resulting in smaller bias between simulations and observations. In contrast, the lower PBL height found in other periods would exaggerate the overestimation in simulated concentrations, given the elevated emissions in JS-prior. We added the analysis **in lines 454-468 in the revised manuscript** and included Figure R1 as **Figure S9 in the revised supplement**. Attributed to the instrument maintenance, moreover, the observation data in January at PAES were relatively insufficient, and the data points were 70% less than those at NJU. Therefore, the contribution of observation at PAES was limited in the multiple regression model.

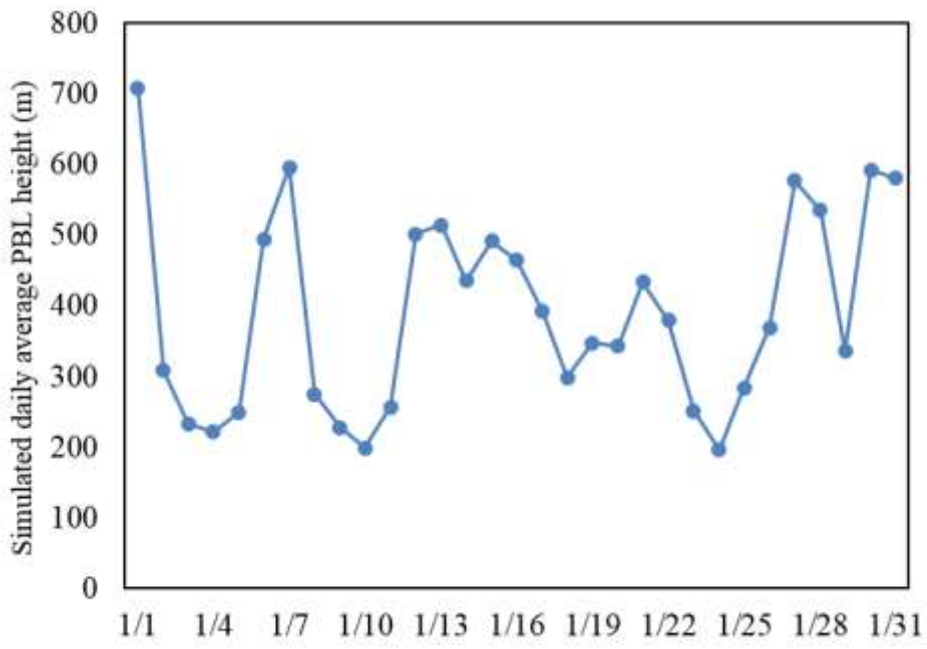

Figure R1. The simulated daily average PBL heights in January 2015 at PAES.

Following the reviewer's suggestion, we excluded the data points in middle and late January (16th -26th) at PAES and re-compared the observed and simulated BC concentrations. As shown in Table R5, the overestimation in CTM was largely reduced when the data were excluded, and the top-down estimate corrected the bias moderately at PAES. We added the discussions **in lines 499-503 in the revised manuscript** and added Table R5 as **Table S6 in the revised supplement**.

Table R5. Statistical indicators for observed and simulated BC concentrations using JS-prior and JS-posterior in January excluding data from 16th to 26th at PAES.

Site	Parameter	JS-prior	JS-posterior
PAES	Average SIM (μg/m^3)	2.86	2.68
	Average OBS (μg/m^3)	2.15	2.15
	NMB (%)	32.95	24.65
	NME (%)	52.61	49.63
	R	0.72	0.74

6. *Lines 456-461: again, could the model bias be due to the lack of biomass burning emissions?*

Response and revisions:

We thank the reviewer's comment. The bigger bias found in July and October at NJU when applying JS-posterior resulted mainly from the limitation of the constraining method. We used observations at two sites to constrain emissions from southern Jiangsu as a whole. Therefore, overestimation and underestimation in concentrations at different sites could not be corrected simultaneously without considering the spatial representation of observation sites, as discussed **in lines 511-516 in the revised manuscript**.

The underestimation in BC concentrations for July and October with JS-prior could be partly due to the lack of biomass open burning emissions. However, such influence was expected to be insignificant (please see our response to Q2), and the impact of the a priori emission input was found limited on the top-down estimation, as discussed **in Section 4.2 in the revised manuscript**.

7. *Tables: There are already many tables in the paper (and maybe not everyone is absolutely necessary). But a table that summarizes the different cases may be helpful for readers to keep track.*

Response and revisions:

We thank and follow the reviewer's comment to make the tables concise. We integrated the original Table 8 to a new Table 3 in the revised manuscript to summarize the modeling performance for different cases. For the original Table 9, moreover, the scaling factors and statistical indicators from the multiple regression model in Case 7 were integrated to Table 5, and the emissions by sector and the relative deviations to JS-posterior in Case 7 were integrated to Table 6. We also moved the original Table 5 that summarizes the emissions from Nanjing and other cities in southern Jiangsu in different cases to Table S9 in the revised supplement.

8. *Table 4 and related discussion on case 3: would the authors expect somewhat different driving conditions and emission factors for automobiles in urban and* *suburban settings? If so, is it still a valid assumption to assume the same scaling factor between NJU and PAES for transportation?*

Response and revisions:

We thank the reviewer's comment. In Case 3, we assumed a same scaling factor for transportation for different cities in southern Jiangsu to avoid the collinearity in the multiple regression model. As the observation data at NJU and PAES were applied to constrain emissions from Suzhou-Wuxi-Changzhou-Zhenjiang city cluster and Nanjing, respectively, the assumption of a same scaling factor at NJU and PAES did not mainly indicate the similar driving conditions or emission factors for automobiles in suburban and urban. Instead, it mainly indicated that the relative changes in emissions from transportation were similar across the cities in southern Jiangsu from 2012 to 2015. As we stated **in lines 591-593 in the revised manuscript**, such assumption is expected to be reasonable, because of the same progress of emission standard implementation (National Standard Stage IV) in southern Jiangsu and the frequent circulation of vehicles among the cities.

References

Wang, X., Wang, Y., Hao, J., Kondo, Y., Irwin, M., Munger, J. W., and Zhao, Y.: Top-down estimate of China's black carbon emissions using surface observations: Sensitivity to observation representativeness and transport model error, Journal of Geophysical Research: Atmospheres, 118, 5781-5795, 10.1002/jgrd.50397, 2013.

Yang, Y., and Zhao, Y.: Quantification and evaluation of atmospheric pollutant emissions from open biomass burning with multiple methods: a case study for the Yangtze River Delta region, China, Atmospheric Chemistry and Physics, 19, 327-348, 10.5194/acp-19-327-2019, 2019.

Reviewer #3

0. *This is a very nice and detailed work to constrain BC emissions in southern Jiangsu. The approach and uncertainty analysis may be applied to other regions. The paper is well written in general, suitable for ACP. Below are a few suggestions to further improve the paper.*

Response and revisions:

We appreciate the reviewer's positive remarks on the importance of the work. Please see the details in the following response and revision list to reviewer's comment.

1. *It would be nice to discuss in the conclusion section the potential of applying the method to other regions.*

Response and revisions:

We thank the reviewer's comment. The method could be applied to constrain the BC emissions for other regions effectively if there are sufficient observation data with satisfying spatiotemporal coverage. We added the statement **in lines 796-799 in the revised manuscript**.

2. *The regression model needs to be further clarified. Are the scaling factors (betta) for each month, day, or hour? Why is there not a term in Eq. 1 for the background (e.g., lateral boundary condition) reflecting the effect of horizontal transport from regions other than southern Jiangsu? Table S3 and Fig. S7 show that the sum of southern Jiangsu contributions is much smaller than 100%, implying a large contribution from regions other than southern Jiangsu.*

Response and revisions:

We thank the reviewer's comment. The scaling factors were obtained for each month and used to constrain the monthly emissions in southern Jiangsu. We clarified it **in lines 235-237 in the revised manuscript**.

Regarding the background reflecting the regional transport, c_{power}, $c_{industry}$, $c_{residential}$ and $c_{transportation}$ in the multiple regression model were simulated by brute-force method in CTM in which emissions from corresponding sector in the third domain were zeroed out. Therefore the contributions of emissions outside southern Jiangsu in the third domain were considered in the model. Moreover, ε reflected the effect of background conditions (e.g., emissions in the first and second domain in CTM and emissions not included in the a priori inventory like those from natural sources). We clarified it **in lines 222-227 and 237-239 in the revised manuscript**. For example, the ε was estimated at 0.96 μg/m^3 in the multiple regression model for April in JS-posterior. By zeroing out the emissions from the third domain in CTM, the monthly contribution from boundary conditions were calculated at 0.76 and 0.77 μg/m^3 at NJU and PAES, respectively. In spite of the modest bias between ε and the estimated contribution of boundary conditions, including ε would reduce the uncertainty of the multiple regression model.

We added the contributions from four sectors in the third domain at the two sites **in Table S5 in the revised supplement**. The total contributions were larger than 50% for all the months and sites except for January. We assumed that the smaller contributions in January resulted partly from the longer lifetime of BC in winter due to less wet deposition. We also identified the transport pathways of air masses sampled at NJU for the four months through cluster analysis of back trajectories with Hybrid Single Particle Lagrangian Integrated Trajectory (HYSPLIT, version 4) model as illustrated in Figures R2. Compared to other months, fewer air masses passed through the third modeling domain in January due to the prevailing northerly wind, implying more contribution from regional transport to the air quality at the site in January. Similar results were found for other region. Jia et al. (2008) estimated that regional transport on average contributed nearly 50% of PM (up to 70% in southerly regions) in winter in three sites in Beijing. Sun et al. (2014) considered the accumulation of local BC emissions and estimated a contribution of 53% from regional transport to BC in Beijing. Given the smaller contribution of emissions within the third domain in January, we acknowledged that the multiple regression model was less effective on identifying the sources of BC in winter by constraining the emissions in southern Jiangsu city cluster alone. We added the discussion **in lines 360-370 in the revised manuscript** and included Figure R2 as **Figure S6 in the revised supplement**.

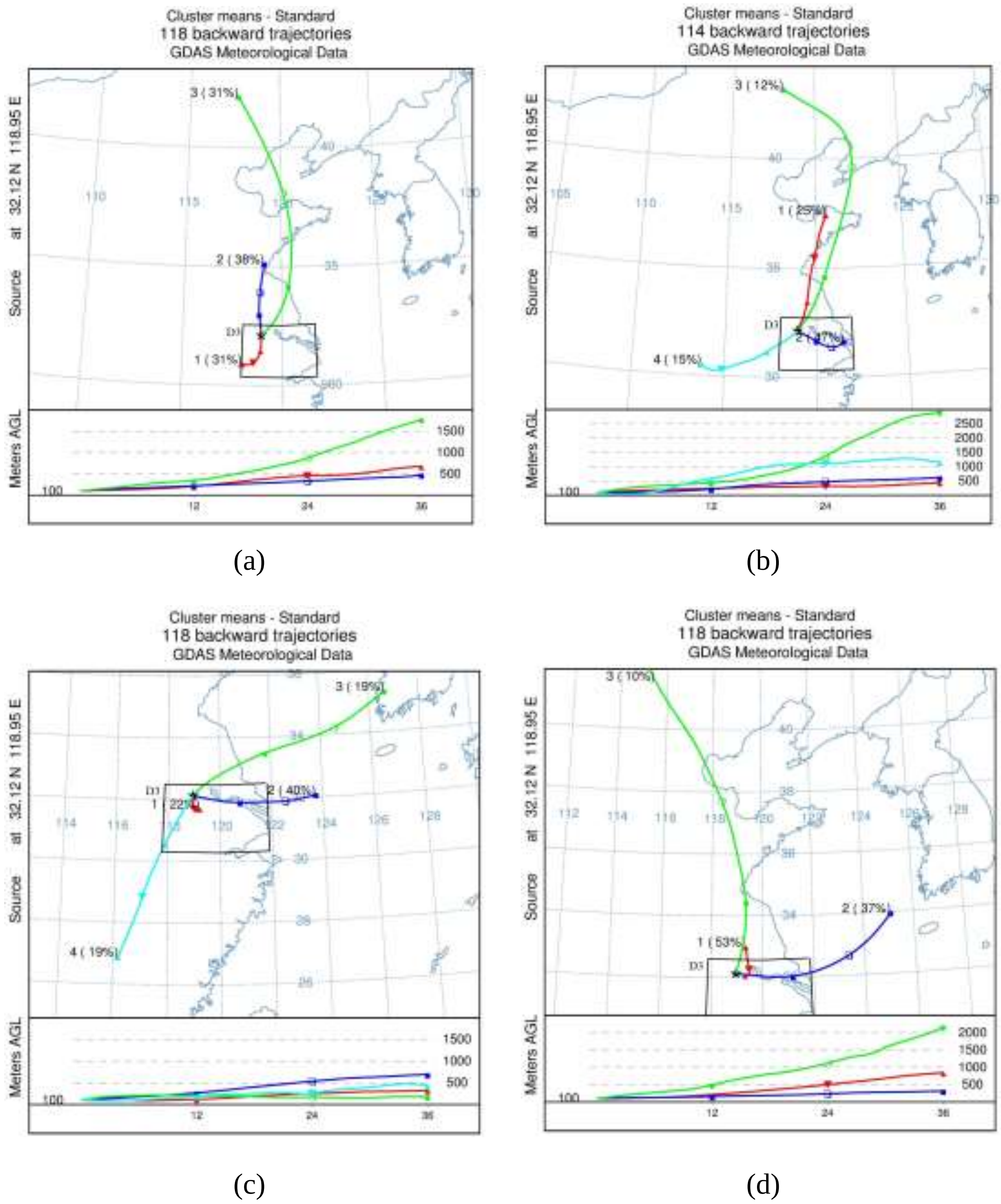

Figure R2. The transport pathways of air masses sampled at NJU based on cluster analysis of back trajectories in HYSPLIT model in January (a), April (b), July (c) and October (d).

3. *The idea of testing the spatial representativeness of measurements is very nice. Given the spatial representativeness difference between the two sites, is it possible to use Case 3 as your best case? Alternatively, it would be nice to improve the regression model by taking into account the transport path, e.g., by basing on WRF modeled winds to design a model that considers the trajectory of air movement. The much higher bias in JS-posterior than JS-prior in Case 1, which is a concern, is related to this spatial representativeness issue.*

Response and revisions:

We thank the reviewer's comment. Among all the cases discussed in the paper, the best CTM performance was obtained in Case 3 in which observations at both sites were used with their difference in spatial representativeness considered in the constraining method. We also appreciate the reviewer's suggestion, which could potentially improve the analysis of spatial representativeness and could be applied with more observation data available in the future. The larger NMEs in July and October at NJU in JS–posterior than JS-prior were related to the spatial representativeness issue, which was discussed **in lines 511-516 in the revised manuscript**.

4. *A clearer discussion of temporal resolution in bottom up inventories and how this resolution affects the top-down constraint will be very helpful.*

Response and revisions:

We thank the reviewer's comment. We derived the hourly bottom-up emission inventory for CTM. The monthly distributions of emissions from power plants and industry plants in JS-prior were dependent on those of electricity generation and typical industrial production, respectively. Such information was investigated by Zhou et al. (2017) according to the official statistics of the country (http://data.stats.gov.cn/). Meanwhile, the real-time monitoring on urban traffic in Nanjing was applied to allocate the temporal distribution of emissions from on-road vehicles in the whole regions in JS-prior. The weekly and hourly distributions of different sources in YRD (Li et al., 2011) were adopted to further allocate emissions in JS-prior. For MEIC-prior, we obtained the monthly emissions directly and applied the same weekly and hourly distributions as JS-prior. We described this **in lines 207-215 in the revised manuscript**. The temporal distributions based on local statistical data were expected to be more reliable in CTM than other information. Regarding the effect of the monthly variation on the constraint method, we compared top-down estimate derived from JS-prior and MEIC-prior in April, respectively, **in Section 4.2 in the revised manuscript**. Similar emission estimation, spatial distribution and modeling performance were found for the two a posteriori emissions, even clear difference existed in the two a priori inventories. The result thus implied the insignificant effect of monthly variation of emissions on the top-down constraint. We discussed this **in lines 667-671 in the revised manuscript**. We did not constrain the hourly emissions in this study and the hourly distribution was thus unchanged in the top-down estimate.

5. *Comparison with near-surface measurements is sensitive to WRF/CMAQ modeled vertical processes, including the number of vertical layers within the PBL, the thickness of the first layer, and the model error in vertical mixing representation. WRF/CMAQ may have some issues with PBL mixing (Liu et al., 2018). Please specify these model setups. Please discuss the potential effect of model vertical resolution/mixing/transport errors on the BC constraint.*

Response and revisions:

We thank the reviewer's comment. The PBL module adopted in WRF 3.4 was ACM2, and the information was added **in line 285 in the revised manuscript**. There were 27 vertical layers in the model, with the heights of 54, 132, 234, 362, 523, 729, 974, 1417, 1887, 2385, 2914, 3900, 4890, 5886, 6885, 7885, 8891, 9907, 10946, 12000, 13070, 14158, 15278, 16441, 17662, 18966 and 20405 m, respectively. The simulated monthly average PBL heights along with the range of hourly simulations at

NJU and PAES in four months were shown in Table R6. Therefore, there were average 5 vertical layers within the PBL. We found the similar result of the low simulated PBL height in WRF/CMAQ model as Liu et al. (2018) and the overestimation of BC concentration at PAES even after top-down constraint may result from it. We added the analysis **in lines 503-507 in the revised manuscript** and included Table R6 as **Table S7 in the revised supplement**.

The effect of vertical distribution on BC emission constraining was evaluated for Asia by Zhang et al. (2015). They repeated the top-down inversions using the OMI retrieval absorption aerosol optical depth (AAOD) based on the CALIOP and GOCART aerosol layer height and found the difference in the optimized BC emissions were less than 30% in April and 10% in October compared to the optimized emissions using the initial GEOS-Chem model. The difference was within the acceptable range compared with up to 500% enhancements in April and 10-50% in October with the top-down constraining. When applying ground observations in this study rather than column concentration in AAOD, the effect of vertical distribution could be smaller.

Table R6. The simulated monthly average PBL heights and the range of hourly simulations at NJU and PAES in four months.

Month	Site	Monthly average PBL (m)	Hourly average PBL (m)
January	NJU	370.25	27.59-1443.64
	PAES	384.56	27.20-1460.07
April	NJU	432.73	28.61-2157.87
	PAES	441.72	28.61-2157.87
July	NJU	381.14	30.70-1617.69
	PAES	431.02	30.02-1975.01
October	NJU	462.57	29.70-2065.97
	PAES	488.30	29.78-2073.46

6. *Table S2 shows that the prevailing winds in all three meteorological sites are southerly or southeasterly. I thought there would be northerly in the cold months (January and October). Please double check.*

Response and revisions:

We thank the reviewer's comment. We checked the simulated and observed wind directions again and found the same result. The NMEs of wind directions were found below 40% at three meteorological stations in January and October, reflecting the robustness of the WRF modeling. In January, the average simulations and observations **in Table S4 in the revised supplement** did not mean that the prevailing winds were southerly. The values were the mean of the northerly wind directions ranging from 0-45^{o} or 315-360^{o}. Taking the wind directions at Hongqiao in January and October as examples, the prevailing winds were northerly and easterly in winter and autumn, respectively, as shown in Figures R3.

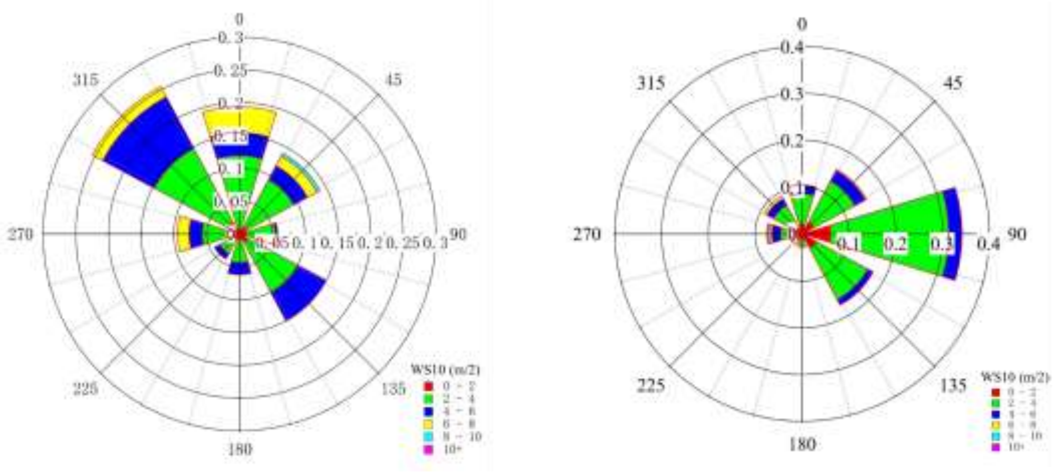

(a) (b)

Figure R3. Wind speeds and directions at Hongqiao in January (a) and October (b).

7. *Some paragraphs are too long and should be splitted, for example, L71-111, L352-388.*

Response and revisions:

We thank the reviewer's comment. As suggested by the reviewer, we split L71-111 in the initial manuscript into two parts, one was about the large uncertainties in bottom-up emission inventories, and the other was the challenge existing in updating BC inventories continuously, **in lines 74-114 in the revised manuscript**. We split L352-388 in the original manuscript and reorganized the paragraphs. One was about the relative change between JS-prior and JS-posterior, and the other was the detailed description about scaling factors for different sectors, **in lines 387-424 in the revised manuscript**.

8. *Abstract – please specify that monthly, sector-level and city-level emissions are optimized.*

Response and revisions:

We thank the reviewer's comment. We followed the suggestion and specified the optimized monthly, sector-level and city-level emissions in **in line 24 in the revised manuscript**.

9. *L22 – "observations," should be "observations" (no comma).*

Response and revisions:

We thank the reviewer's reminder and deleted the comma **in line 23 in the revised manuscript**.

10. *Abstract – please specify that WRF/CMAQ is used.*

Response and revisions:

We thank the reviewer's reminder and specified the WRF/CMAQ model **in lines 21-22 in the revised manuscript**.

11. *L214 – is there is term for background (due to horizontal transport)?*

Response and revisions:

We thank the reviewer's comment. ε reflected the effect of emissions from background conditions, which was added **in lines 237-239 in the revised manuscript**. (please also see our response to Q2).

12. *L218 – "domain-wide" – here you optimize the southern Jiangsu emissions, not the domain-wide emissions. Also, as suggested above, an improved regression model may be used to better account for spatial representativeness of measurements.*

Response and revisions:

We thank the reviewer's comment and revised the words for β_1-β_4 **in lines 235-237 in the revised manuscript**. We appreciate the reviewer's suggestion to improve the multiple regression model and it could be applied with more observation data available in the future to better consider spatial representativeness.

13. *L256 – "coordinated" should be "coordinate"*

Response and revisions:

We thank the reviewer's reminder and corrected the word **in line 281 in the revised manuscript**.

14. *L274-288 – please specify the temporal resolution of bottom up emissions.*

Response and revisions:

We thank the reviewer's comment. We specified the temporal distributions of two bottom-up emission inventories used in CTM **in lines 207-215 in the revised manuscript**. The monthly distributions of emissions from power plants and industry plants in JS-prior were dependent on those of electricity generation and typical industrial production, respectively. Such information was investigated by Zhou et al. (2017) according to the official statistics of the country (http://data.stats.gov.cn/). The real-time monitoring on urban traffic in Nanjing was applied to allocate the temporal distribution of emissions from on-road vehicles in the whole regions in JS-prior. The weekly and hourly distributions of different sources in the Yangtze River Delta (Li et al., 2011) were directly adopted to further allocate the emissions in JS-prior. For MEIC-prior, we obtained the monthly emissions and applied the same weekly and hourly distributions as JS-prior. The temporal allocations based on local statistical data were expected to be more reliable in CTM.

15. *L283-285 – do you remove emissions in the whole domain, or just southern Jiangsu cities?*

Response and revisions:

We thank the reviewer's comment. We removed emissions in the whole third domain, and it was specified **in lines 308-310 in the revised manuscript**.

16. *L288 – "Scenarios B and S" should be "Scenarios B and S1-S4"*

Response and revisions:

We thank the reviewer's reminder and revised it **in line 313 in the revised manuscript**.

17. *L324 – "double" should be "twice"*

Response and revisions:

We thank the reviewer's comment and corrected the word **in line 349 in the revised manuscript**.

18. *L340 – "VIF smaller than 10" – the VIF values in the table are much smaller than 10.*

Response and revisions:

We thank the reviewer's reminder and revised it **in lines 374-376 in the revised manuscript**.

19. *L386-388 – this sentence is not clear*

Response and revisions:

We thank the reviewer's comment. Based on the bottom-up approach, Huang et al. (in preparation) incorporated detailed information and changes of individual sources, and estimated BC emissions for Nanjing from 2012 to 2015. The emissions in 2015 were estimated to decrease by 60% compared to those in 2012, and this relative change was close to that for the southern Jiangsu (a 50% reduction from JS-prior to JS-posterior) found in this study. The top-down method could thus capture the changes in emissions due to improved control measures. We revised the sentence **in lines 395-398 in the revised manuscript**.

20. *L418-442 – A figure would be much better than a table for this type of analysis.*

Response and revisions:

We thank the reviewer's comment. **Figures 3 and 4 in the revised manuscript** illustrated the simulated BC concentrations based on JS-prior and observations in four months at NJU and PAES, respectively. The analysis mentioned by the reviewer was reflected in those figures.

21. *L426 – what do you mean by "commonly"? The wording may be improved.*

Response and revisions:

We thank the reviewer's reminder and replaced the word commonly with generally **in line 472 in the revised manuscript**.

22. *L443-446 – The increased bias from JS-prior to JS-posterior at NJU should be discussed in more detail.*

Response and revisions:

We thank the reviewer's comment. The increased bias from JS-prior to JS-posterior in July and October at NJU and the detailed analysis was mentioned **in lines 508-516 in the revised manuscript**. It resulted mainly from the limitation of current multiple regression model that overestimation and underestimation in concentrations at different sites could hardly be corrected simultaneously without further improvement in spatial distribution of emissions.

23. *L464 – some cases are for other months.*

Response and revisions:

We thank the reviewer's comment. The sensitivities to observation and bottom-up emission input were evaluated in April (Cases 2-5). We evaluated the near linearity between emissions and concentrations in July and October as the two months were identified as the months with the most and least impact from precipitation suggested by simulated wet deposition to emission ratio. The impacts of simulated wet deposition and satellite-derived accumulated precipitation on top-down estimate were evaluated in July (Case 6-7). We had specified it **in lines 518-525 in the revised manuscript**.

24. *L551 – "initial" should be "a priori". Please revise throughout the text.*

Response and revisions:

We thank the reviewer's reminder and revised it throughout the text.

25. *L573-604 – the paragraph contains multiple messages, and is better to be splitted.*

Response and revisions:

We thank the reviewer's comment. As suggested, the smaller difference in BC emissions and simulated concentrations between JS-posterior and MEIC-posterior were split **in lines 639-666 in the revised manuscript**. The effect of the a priori bottom-up emission inventories on top-down estimate was summarized in another paragraph **in lines 667-671 in the revised manuscript**.

26. *Figs. S8-11 – the dates of precipitation are also not very well simulated.*

Response and revisions:

We thank the reviewer's comment and delete the evaluation of simulated precipitation dates **in lines 703-704 in the revised manuscript**. Considering the large discrepancy between simulated and observed precipitation, we conducted Case 7 to screen satellite-derived precipitation and compared the top-down estimates in two cases.

27. *L701 – "insignificant" should be "modest"*

Response and revisions:

We thank the reviewer's reminder and revised it **in line 763 in the revised manuscript**.

28. *L715-717 – the increased bias at NJU should be mentioned.*

Response and revisions:

We thank the reviewer's comment and mentioned the increased bias **in lines 779-780 in the revised manuscript**.

29. *L735-737 – it would be extremely difficult to use satellite AOD to constrain BC emissions.*

Response and revisions:

We thank the reviewer's comment and deleted the texts in the revised manuscript.

References

Gilardoni, S., Vignati, E., and Wilson, J.: Using measurements for evaluation of black carbon modeling, Atmospheric Chemistry and Physics, 11, 439-455, 10.5194/acp-11-439-2011, 2011.

Jia, Y., Rahn, K. A., He, K., Wen, T., and Wang, Y.: A novel technique for quantifying the regional component of urban aerosol solely from its sawtooth cycles, Journal of

Geophysical Research, 113, 10.1029/2008jd010389, 2008.

Li, L., Chen, C. H., Fu, J. S., Huang, C., Streets, D. G., Huang, H. Y., Zhang, G. F., Wang, Y. J., Jang, C. J., Wang, H. L., Chen, Y. R., and Fu, J. M.: Air quality and emissions in the Yangtze River Delta, China, Atmos. Chem. Phys., 11, 1621–1639, doi:10.5194/acp-11-1621-2011, 2011.

Liu, M., Lin, J., Wang, Y., Sun, Y., Zheng, B., Shao, J., Chen, L., Zheng, Y., Chen, J., Fu, T.-M., Yan, Y., Zhang, Q., and Wu, Z.: Spatiotemporal variability of NO_2 and $PM_{2.5}$ over Eastern China: observational and model analyses with a novel statistical method, Atmospheric Chemistry and Physics, 18, 12933-12952, 10.5194/acp-18-12933-2018, 2018.

Matsui, H., Koike, M., Kondo, Y., Oshima, N., Moteki, N., Kanaya, Y., Takami, A., and Irwin, M.: Seasonal variations of Asian black carbon outflow to the Pacific: Contribution from anthropogenic sources in China and biomass burning sources in Siberia and Southeast Asia, Journal of Geophysical Research-Atmospheres, 118, 9948-9967, 10.1002/jgrd.50702, 2013.

Sun, Y., Jiang, Q., Wang, Z., Fu, P., Li, J., Yang, T., and Yin, Y.: Investigation of the sources and evolution processes of severe haze pollution in Beijing in January 2013, Journal of Geophysical Research-Atmospheres, 119, 4380-4398, 10.1002/2014jd021641, 2014.

Wang, X., Wang, Y., Hao, J., Kondo, Y., Irwin, M., Munger, J. W., and Zhao, Y.: Top-down estimate of China's black carbon emissions using surface observations: Sensitivity to observation representativeness and transport model error, Journal of Geophysical Research-Atmospheres, 118, 5781-5795, 10.1002/jgrd.50397, 2013.

Zhang, L., Henze, D. K., Grell, G. A., Carmichael, G. R., Bousserez, N., Zhang, Q., Torres, O., Ahn, C., Lu, Z., Cao, J., and Mao, Y.: Constraining black carbon aerosol over Asia using OMI aerosol absorption optical depth and the adjoint of GEOS-Chem, Atmospheric Chemistry and Physics, 15, 10281-10308, 10.5194/acp-15-10281-2015, 2015.

Zhou, Y., Zhao, Y., Mao, P., Zhang, Q., Zhang, J., Qiu, L., and Yang, Y.: Development of a high-resolution emission inventory and its evaluation and application through air quality modeling for Jiangsu Province, China, Atmospheric Chemistry and Physics, 17, 211-233, 10.5194/acp-17-211-2017, 2017.

Top-down estimate of black carbon emissions for city cluster using ground observations: A case study in southern Jiangsu, China

Xuefen Zhao[1], Yu Zhao[1, 2*], Dong Chen[1], Chunyan Li[3], Jie Zhang[3]

1. State Key Laboratory of Pollution Control and Resource Reuse and School of the Environment, Nanjing University, 163 Xianlin Ave., Nanjing, Jiangsu 210023, China

2. Jiangsu Collaborative Innovation Center of Atmospheric Environment and Equipment Technology (CICAEET), Nanjing University of Information Science and Technology, Jiangsu 210044, China

3. Jiangsu Provincial Academy of Environmental Science, 176 North Jiangdong Rd., Nanjing, Jiangsu 210036, China

*Corresponding author: Yu Zhao

Phone: 86-25-89680650; email: *yuzhao@nju.edu.cn*

Abstract

We combined a chemistry transport model (~~CTM~~the Weather Research and Forecasting and the Models-3 Community Multi-scale Air Quality Model, WRF/CMAQ), a multiple regression model and available ground observations~~,~~ to optimize ~~derive top-down estimate of~~ black carbon (BC) emissions at monthly, emission sector and city cluster level. We derived top-down emissions and ~~to~~ reduced deviations between simulations and observations for southern Jiangsu city cluster, a typical developed region of eastern China. Scaled from a high-resolution inventory for 2012 based on changes in activity levels, the BC emissions in southern Jiangsu were calculated at 27.0 Gg/yr for 2015 (JS-prior). The annual mean concentration of BC at Xianlin Campus of Nanjing University (NJU, a suburban site) was simulated at 3.4 μg/m^3, 11% lower than the observed 3.8 μg/m^3. In contrast, it was simulated at 3.4 μg/m^3 at Jiangsu Provincial Academy of Environmental Science (PAES, an urban site), 36% higher than the observed 2.5 μg/m^3. The discrepancies at the two sites implied the uncertainty of the bottom-up ~~-~~inventory of BC emissions. Assuming a near-linear response of BC concentrations to emission changes, we applied a multiple regression model to fit the hourly surface concentrations of BC at the two sites, based on the detailed source contributions to ambient BC levels from brute-force simulation. Constrained with this top-down method, BC emissions were estimated at 13.4 Gg/yr (JS-posterior), 50% smaller than the bottom-up estimate, and stronger seasonal variations were found. Biases between simulations and observations were reduced for most months at the two sites when JS-posterior was applied. At PAES, in particular, the simulated annual mean ~~was reduced~~declined ~~elevated~~ to 2.6 μg/m^3 and the annual normalized mean error (NME) decreased from 72.0% to 57.6%. However, application of JS-posterior slightly enhanced NMEs in July and October at NJU where simulated concentrations with JS-prior were lower than observations, implying that reduction in total emissions could not correct ~~CTM~~ modeling underestimation. The effects of observation site including numbers and spatial representativeness~~ of observation sites~~ on top-down estimate were further quantified. The best ~~CTM~~ modeling performance was obtained when observations of both sites were used with their difference in spatial functions considered in emission constraining. Given the limited BC observation data in the area, therefore, more measurements with better spatiotemporal coverage were recommended for constraining BC emissions effectively. Top-down estimates derived from JS-prior and the Multi-resolution Emission Inventory for China (MEIC) were compared to test the sensitivity of the method to the a ~~initial~~ priori emission input. The differences in emission levels, spatial distributions and ~~CTM~~ modeling performances were largely reduced after constraining, implying that the impact of the a ~~initial~~ priori inventory was limited on top-down estimate. Sensitivity analysis proved the rationality of near linearity assumption between emissions and concentrations, and the impact of wet deposition on the multiple regression model was demonstrated moderate through data screening based on simulated wet deposition and satellite-derived precipitation.

1 Introduction

Black carbon (BC), alternatively referred as elemental carbon (EC), is a~~n~~ crucial component of atmospheric particle and comes mainly from incomplete combustion of fossil fuels and biomass. BC has adverse effect on human health as it absorbs harmful volatile organic compounds like polycyclic aromatic hydrocarbons (Dachs and Eisenreich, 2000). Furthermore, BC contributes to global warming by intercepting and absorbing sunlight (Jacobson, 2001; Ramanathan and Carmichael, 2008). Bond et al. (2013) assessed that the global average radiative forcing of BC was +1.1 W/m^2 (90% confidence interval: 0.17-2.1 W/m^2), which was more than two-thirds of that from CO_2 (+1.56 W/m^2). Since BC remains for only a few days in the atmosphere, it is an effective way to mitigate climate warming in the short term by reducing BC emissions. However, due to lack of sufficient understanding of major emission sources, the effect of BC on regional climate was not fully quantified by models.

BC emission inventories are traditionally developed with the bottom-up method based on activity levels and emission factors. Previous studies of chemistry transport modeling (CTM) based on emission inventories found large discrepancies between simulated and observed BC concentrations. Koch et al. (2009) found that sixteen models applied in the AeroCom aerosol model inter-comparison project underestimated surface BC levels by a factor of 2-3. Hu et al. (2016) found that CTM significantly underestimated the peak surface concentrations of BC over northwestern United States, likely due to missing strong local fire events in fire emissions. Moreover, large differences existed in various bottom-up emission inventories, particularly for China with large energy consumption, complicated emission source categories, and fast changes in emission characteristics. BC emissions in China for 2001 and 2006 in the Regional Emission inventory in ASia (REAS 2.1, Kurokawa et al., 2013) were smaller than those in the Intercontinental Chemical Transport Experiment-Phase B (INTEX-B, Zhang et al., 2009), but the growth rate of BC emissions in REAS 2.1 was larger than that in INTEX-B (30% versus 15%) for the ~~five~~ six years. Ohara et al. (2007) evaluated the inter-annual trend in China's BC emissions with constant emission factors, and found that the national emissions continuously decreased by 23% from 1990 to 2000. In contrast, Lei et al. (2011) suggested a much smaller inter-annual variability with the peak annual emissions found in 1996 for the same period. The differences resulted largely from the use of activity levels from various data sources, especially for residential biofuel combustion. The gaps between different studies implied potentially large uncertainties in BC bottom-up emission inventories. The uncertainties of BC emission estimates for China were reported at ±484%, ±208%, and ±98% by Streets et al. (2003), Zhang et al. (2009), and Lu et al. (2011), respectively. Due to lack of sufficient local field tests, emission factors were commonly taken from foreign studies with big variety depending on fuel and combustion condition (Bond et al., 2004; Cao et al., 2006; Lei et al., 2011; Qin and Xie, 2012; Streets et al., 2003; Streets et al., 2001; Zhang et al., 2009). It was also difficult to obtain accurate and detailed activity data, particularly for the main sources of BC including small industries (e.g., coke and brick production), off-road transportation, and residential solid fuel combustion.

Besides the large uncertainty in emission estimation, challenges existed as well in updating BC inventories continuously (Hong et al., 2017; Lu et al., 2011; Xia et al., 2016; Zhao et al., 2013). To beat severe air pollution, China has been conducting series of measures in energy conservation and emission control, leading to dramatic changes in energy structure, emission factors and removal rates of air pollutant control devices (Zhao et al., 2014). Such changes could be partly tracked by continuous emission monitoring system (CEMS) that was commonly installed at big industrial enterprises. Large fractions of BC emissions, however, came from medium and small sources, and their most recent improvements in manufacturing technologies and emission controls were relatively difficult to be obtained timely and efficiently.

Given above limitations in bottom-up inventories, different top-down approaches were applied to evaluate BC emissions. For example, Cohen and Wang (2014) presented a Kalman filter technique to estimate the global BC emissions based on satellite-derived radiances and surface concentrations from global and regional networks. The adjoint-based 4-D variational approach was also applied to constrain the bottom-up BC emissions at the global or national scales (Zhang et al., 2015; Xu et al., 2013; Guerrette et al., 2017). A near-linear response of BC concentrations to emission changes was generally assumed at national (Fu et al., 2012; Kondo et al., 2011; Wang et al., 2013) and regional scales (Li et al., 2015; Wang et al., 2011), due to its weak activity in atmospheric chemistry reaction. The ratio of observed to simulated concentration can be used as a scaling factor to correct BC emissions. Kondo et al. (2011) made continuous measurement of BC concentrations for a full year on a remote island in East China Sea. With the data strongly affected by emissions from China identified and those largely influenced by wet deposition excluded, they estimated China's annual anthropogenic BC emissions at 1.92 TgC/yr. Wang et al. (2013) verified this linearity by conducting sensitivity simulation in which emissions were increased by 50%. After excluding observation data of heavy pollution and strong precipitation events at five Chinese sites, they calculated China's annual BC emissions at 1.80 TgC/yr. The results of both studies were close to a bottom-up estimate at 1.81 TgC/yr by Zhang et al. (2009). Based on observations at 10 Chinese background and rural sites, Fu et al. (2012) applied a multiple regression model and CTM to quantify China's BC emissions. They calculated the total emissions at 3.05 TgC/yr, 59% larger than those by Zhang et al. (2009). Using similar approach, Li et al. (2015) estimated BC emissions to be 34% larger than bottom-up inventory in Pearl River Delta in south China by Zheng et al. (2012). Park et al. (2003) used the multiple linear regression to fit the Interagency Monitoring of Protected Visual Environments (IMPROVE) data and estimated that BC emissions from fossil fuel and biofuel burning in the United States should be increased by 15%. Combining a general circulation model simulation and the receptor modeling approach, Verma et al. (2017) constrained BC emissions over India based on the scaling factor (the ratio of simulated to observed BC concentration).

To our knowledge, limitations remained in the assessment of BC emissions based on the top-down approach. Current available studies focused mainly on global or national scale, and few evaluations could be found for city clusters. In aims of examining emission control policies and quantifying impacts of BC on local climate and air quality, there was a strong need for studies at city cluster scale that require ground observation and emission inventory with improved details. Regarding measurement data, monthly or annual means were commonly used in previous studies, and information of heavy-polluted events were lost when targeting a local scale. In general, observations at a higher temporal resolution were considered as an important means to effectively reduce uncertainties (Matsui et al., 2013; Wang et al., 2013; Gilardoni et al., 2011). Moreover, it was somewhat arbitrary to differentiate emissions by sector in previous top-down estimates, attributed to lack of detailed information on source categories from bottom-up inventories. The method was thus insufficient to make substantial improvement on emission evaluation by sector, or to clearly stress the direction of further revisions on bottom-up inventories.

In this work, therefore, we integrated CTM, multiple regression model and available hourly ground observations to provide top-down constraint of BC emissions and to reduce deviations between simulations and observations at city cluster scale. We selected southern Jiangsu city cluster including cities of Suzhou, Wuxi, Changzhou, Zhenjiang, and Nanjing, a typical region with large population and economy in the Yangtze River Delta (YRD), China (see the geographic location and cities in Figure S1 in the supplement). Given its intensive industry and energy consumption, the city cluster was regarded as one of the largest BC emission sources in eastern China and BC emissions from this region accounted for nearly half of the total emissions in Jiangsu (Zhou et al., 2017). The heavy air pollution was found in the region: the annual averages of fine particle ($PM_{2.5}$) concentrations in all the cities exceeded the National Ambient Air Quality Standard (NAAQS, 35 μg/m^3) in 2012. Under the pressure of air quality improvement, Jiangsu conducted aggressive actions of emission control, leading to 20% reduction in the annual average of $PM_{2.5}$ concentration from 2013 to 2015. Based on a provincial bottom-up emission inventory, we estimated the contributions to BC concentrations by sector at two ground observation sites through the brute-force method in CTM. The results, together with observed ambient BC concentrations, were incorporated in a multiple regression model to derive the top-down estimate of BC emissions for southern Jiangsu city cluster. The advantage of top-down estimate against bottom-up inventory was then judged by CTM and ground observations. The factors that would potentially influence the top-down estimate were also evaluated, including number and spatial representativeness of observation sites, and the a ~~initial~~ priori bottom-up emission input. The near-linearity assumption in ~~uncertainties of~~ the multiple regression model and the effect of wet deposition on the top-down estimate were finally evaluated ~~including the influence of precipitation and the near linear assumption between BC~~

~~emissions and concentrations~~.

2 Data and method

2.1 Bottom-up inventories of BC emissions

Two bottom-up emission inventories at different spatial scales were used in this work. At the national scale, the Multi-resolution Emission Inventory for China (MEIC, http://www.meicmodel.org/) was developed by Tsinghua University, with an original horizontal resolution at 0.25°×0.25°. At the provincial scale, Zhou et al. (2017) collected the best available information of industrial sources in Jiangsu and developed an inventory with higher resolution at 3×3 km. The latter was proved to be more supportive in air quality simulation at city cluster scale (Zhou et al., 2017; Zhao et al., 2017). In both inventories, anthropogenic BC emissions for 2012 came from four major sectors: power generation, industry, residential sources and transportation. The national and provincial inventories for 2015 (mentioned respectively as MEIC-prior and JS-prior hereinafter) were obtained using a simple scaling method based mainly on changes in activity levels (energy consumption and industrial production, etc) between the four years. Table S1 in the supplement summarizes the data sources of activity levels and the scaling factors by sector in JS-prior. As MEIC-prior includes only four major sectors, the scaling factor for each sector was calculated as the average of those for subcategories within the sector. Potential changes in BC emission factors from 2012 to 2015, e.g., those attributed to varied manufacturing technologies and/or penetrations of emission control devices, were not considered in the calculation. The implication and uncertainty from that simplified emission scaling method will be further discussed in Section 4.~~3~~2. ~~The temporal distribution of the emissions was dependent on that of activity levels by source category.~~The monthly distributions of emissions from power plants and industry plants in JS-prior were dependent on those of electricity generation and typical industrial production, respectively. Such information was investigated by Zhou et al. (2017) according to the official statistics of the country (http://data.stats.gov.cn/). ~~and directly adopted in this work.~~ ~~Meanwhile,~~ ~~t~~The real-time monitoring on urban traffic in Nanjing was applied to allocate the temporal distribution of emissions from on-road vehicles in the whole regions in JS-prior. The weekly and hourly distributions of ~~different~~other sources were taken from ~~in the Yangtze River Delta (~~Li et al., (~~-~~2011)~~. were directly adopted to further allocate emissions in JS-prior.~~ ~~As f~~For MEIC-prior, we obtained the monthly emissions directly and ~~used~~ applied the same weekly and hourly distributions as JS-prior. ~~The temporal allocations based on local statistical data were expected to be more reliable in CTM.~~

批注 [zy1]: 这里需要举例说明，例如典型源的排放精确到月？ 看 Zhou 的原文。但注意用语简练

2.2 Top-down emission estimation with multiple regression model

The top-down emissions of BC in southern Jiangsu (mentioned as JS-posterior hereinafter) were estimated with a multiple regression model using ground observations as constraint. The regression model matched BC contributions by sector (calculated through CTM) against measured ambient hourly BC concentrations:

$$c_{obs} = \beta_1 c_{power} + \beta_2 c_{industry} + \beta_3 c_{residential} + \beta_4 c_{transportation} + \varepsilon \quad (1)$$

where c_{obs} is the vector of observed hourly BC concentrations.~~;~~ c_{power}, $c_{industry}$, $c_{residential}$, and $c_{transportation}$ are the vectors of BC concentrations contributed by power generation, industry, residential sources and transportation in southern Jiangsu ~~along with~~and nearby ~~cities~~ regions (the third domain of air quality modeling, as described later in Section 2.3), respectively, and they were simulated using the brute-force method as described in Section 2.3. Southern Jiangsu and nearby cities were considered as a whole in the multiple regression model ~~as a whole~~ based on ~~the~~an assumption of ~~the consistence~~ similar ~~of~~ implementation of air~~ed~~ pollution control measures ~~there~~ for the two regions. ~~Regarding the uncertainty of the assumption due to the fact that different local governments could take different policies from 2012 to 2015,~~ Tables S2 and S3 in the supplement summarize respectively ~~we evaluated~~ the ~~decrease trend~~reduction rates ~~of~~ in BC emissions estimated by ~~in~~ MEIC and ~~—~~those in observed ~~–~~PM$_{2.5}$ ~~observations~~concentrations for~~ during~~ recent~~these~~ years ~~in~~ for southern Jiangsu and nearby cities~~ (limited BC observations in those regions)~~. ~~as shown in Tables S2 and S3 in the supplement.~~ The ~~bias~~discrepancies in reduction rates between the two regions were found less than 6% and 7% for monthly BC emissions and annual PM$_{2.5}$ concentrations, respectively, implying the similar progress of emission control and air quality improvement.~~ of relative reduction of monthly emissions between two regions was less than 6% and analogue bias of PM$_{2.5}$ observations was 7%, implying the rationality of the assumption.~~~~;~~ β_1-β_4 are the ~~domain-wide~~ scaling factors obtained by sector in the multiple regression model and were applied to optimize southern Jiangsu emissions to best match observations for each month.~~;~~ ~~and~~ ε is the error vector of the model, reflecting the effect of background conditions (e.g., emissions~~ in~~ outside the third domain in CTM and ~~the first and second domain in CTM)~~emissions not included in the a priori inventory like those from natural sources). Before applying observations and simulated contributions by sector in the multiple regression model,~~ the~~ data screening was conducted following the criterions: the periods lack of observation data, those for which the contribution of each emission sector was simulated to be smaller than zero through the brute-force method~~ with CTM~~, and those for which the sum of contributions of all the four sectors was larger than 100%~~ with CTM~~. The data screening helped to ~~minimize~~reduce the uncertainty of CTM in the multiple regression model.

As BC is not one of the six regulated air pollutants in the NAAQS, it was a big challenge to obtain observation data with high temporal resolution in most cities of southern Jiangsu. For the whole year 2015, hourly ambient BC concentrations were available at two sites in Nanjing, the capital of Jiangsu. As illustrated in Figure 1, one is a suburban site located in the Xianlin Campus of Nanjing University in northeast Nanjing (NJU), and the other is an urban site in Jiangsu Provincial Academy of Environmental Science (PAES). At both sites, BC was sampled and analyzed hourly with semi-continuous carbon analyzer (Model-4, Sunset Lab, USA). Details of the

带格式的: 下标

带格式的: 下标

带格式的: 下标

measurement approach were described in Chen et al. (2017). The statistics of observed ambient BC concentrations at the two sites are shown in Figure S2 in the supplement. The annual average BC concentrations (calculated as the mean of January, April, July and October) were 3.83 and 2.47 μg/m^3 at NJU and PAES, respectively. The hourly average BC observations ranged 0.06-17.65 μg/m^3 and 0.22-19.76 μg/m^3 at NJU and PAES, respectively. The values were similar to those observed in the Guanzhong basin (0.4-23.1μg/m^3), the Pearl River Delta region (1-13 μg/m^3) and the Beijing-Tianjin-Hebei region (2-32 μg/m^3) (Li et al., 2016). Much higher BC concentrations were observed in autumn and winter at both sites, with the monthly means at 3.96 and 5.44 μg/m^3 at NJU and 3.62 and 2.80 μg/m^3 at PAES, respectively.

The scaling factors derived from Eq. (1) were used to constrain BC emissions in southern Jiangsu in –JS-prior from a top-down perspective by assuming a near-linear relation between changes in BC concentrations and emissions:

$$E_{JS-posterior} = \beta_1 E_{power} + \beta_2 E_{industry} + \beta_3 E_{residential} + \beta_4 E_{transportation} \quad (2)$$

where $E_{JS\text{-}posterior}$ is the vector of the total BC emissions from the top-down approach; E_{power}, $E_{industry}$, $E_{residential}$ and $E_{transportation}$ are the vectors of BC emissions from power generation, industry, residential sources and transportation, respectively, in JS-prior.

2.3 Air quality simulation

We used the Models-3 Community Multi-scale Air Quality (CMAQ) version 4.7.1 to simulate ambient BC concentrations. As shown in Figure 1, three nested domains were applied with horizontal resolutions of 27, 9, and 3 km, respectively, on a Lambert Conformal Conic projection centered at (110°E, 34°N). The mother domain (D1, 177×127 cells) covered most parts of China and other surrounding countries. The second domain (D2, 118×121 cells) covered Jiangsu, Anhui, Zhejiang, Shanghai, and parts of other provinces in China–. The third domain (D3, 133×73 cells) covered Shanghai, part of Anhui province and the city cluster in southern Jiangsu. There were 27 vertical levels from the ground surface up to 50 hPa on terrain-following coordinate~~d~~. The simulations were conducted for January, April, July and October to represent four typical seasons in 2015. A 5-day spin-up period of each month was applied to minimize the influence of initial conditions in the simulations.

Meteorological fields were simulated by the Weather Research and Forecasting Model (WRF) version 3.4. ~~and~~ ACM2 planetary boundary layer (PBL) mixing scheme, the carbon bond gas-phase mechanism (CB05) and AERO5 aerosol module were adopted in WRF/CMAQ model. Relevant details of model configuration can be found in Zhou et al. (2017). Statistical indicators including averages of simulations and observations, bias, normalized mean bias (NMB), normalized mean error (NME), root mean squared error (RMSE) and index of agreement (IOA) were applied to evaluate the modeling performance of WRF (Baker et al, 2004; Zhang et al., 2006). Ground observation data at 1 or 3 h interval at meteorological stations including Lukou, Hongqiao and Liyang stations in the third domain (labeled in Figure 1) were taken from National Climatic Data Center (NCDC). The statistical indicators for temperature at 2 m (T2) and relative humidity at 2 m (RH2), wind speed and direction at 10 m (WS10 and WD10) for the four typical months in 2015 are summarized in Table ~~S2~~ S4 in the supplement. Discrepancies between ground observations and WRF modeling were within acceptable range (Emery et al., 2001).

To make it applicable in our CTM, MEIC-prior was downscaled into grid systems of each modeling domain~~,~~ based on the spatial distributions of gross domestic product (GDP, for power generation and industrial emissions) and population (for residential and transportation emissions) at a horizontal resolution of 1×1 km. The downscaled MEIC-prior was used for the first, the second domains and the regions outside Jiangsu of the third domain~~s~~, while JS-prior was applied for the Jiangsu region of the third domain. ~~After applying the temporal distribution of the emissions discussed in Section 2.1, the hourly bottom-up emission inventories were used in CTM. Compared with larger temporal resolution like monthly or annual, the hourly simulated concentrations generated from hourly emissions in CTM could evaluate the~~

批注 [zy2]: 但这些研究中的 hourly resolution 指的是观测浓度还是基于时变化排放模拟的浓度？

~~modeling performance more accurately and reduce uncertainties of top-down method more effectively (Matsui et al., 2013; Wang et al., 2013; Gilardoni et al., 2011). Wang at al., (2013) compared the two methods using monthly and hourly temporal resolutions as constraint respectively, and concluded that the latter one should be a better choice to derive the top-down emissions of BC because it could avoid being greatly affected by outliers or missing data.~~ Brute-force method was applied to estimate contributions to ambient BC concentrations by sector. Five scenarios were designed in this study: Scenario B (the base scenario) in which emissions from all sources in the third domain were included, and Scenarios S1, S2, S3, and S4 in which BC emissions from power generation, industry, residential sources and transportation in the whole third domain were zeroed out, respectively. We compared simulated BC concentrations in S1, S2, S3 and S4 with those in Scenario B in four months at two sites, and the contributions from four major emission sectors to ambient BC levels were determined as the differences in simulated concentrations between Scenarios B and S1-4.

3 Results

3.1 Bottom-up emission estimate

The total annual BC emissions of JS-prior were estimated at 26.99 Gg for southern Jiangsu city cluster in 2015, including 0.18 Gg from power generation, 17.67 Gg from industry, 3.80 Gg from residential sources and 5.33 Gg from transportation, as shown in Figure 2. Accounting for 66% of total annual emissions, industry was identified as the dominant contributor to BC, followed by transportation (20%) and residential sources (14%). Although the policies of energy conservation and emission control have been conducted for years, there were still a number of small facilities with low operation temperatures and combustion efficiencies in southern Jiangsu, leading to a large amount of BC from incomplete combustion. When scaling emissions from 2012 to 2015, in addition, improvements in emission controls were not taken into account, such as elevated combustion technologies and enhanced use of dust collectors. The potential reductions in net emission factors for major factories, therefore, were not well quantified, and the emissions from industry could be overestimated. Emissions from power generation were few, resulting from relatively high combustion efficiency of pulverized boilers and large penetrations and removal rates of dust collectors. Besides the annual total, the emissions of four months (January, April, July and October) were also estimated and limited seasonal differences were found as shown in Figure 2.

Figure S3 in the supplement shows the spatial distribution of annual BC emissions in JS-prior. For power generation and industry sectors, latitude and longitude of each plant were applied to allocate BC emissions, and the outstandingly high emissions shown in the map indicated the existence of big power and industrial plants. For residential sources, large emissions were found in the regions with intensive population. Emissions from transportation were mainly distributed along the road net and downtown regions in southern Jiangsu cities (see the geographic locations of downtowns in Figure S1 in the supplement), slightly overlapping with those from residential sources.

3.2 Top-down emission estimate

The time series of BC concentrations contributed by various sectors (*c* in Eq. (1)) were simulated with CTM and illustrated in Figures S4 and S5 in the supplement for NJU and PAES, respectively. Among all the sectors, the largest seasonal variation in BC contribution was found for residential sources. The average concentrations contributed by this sector in January reached 0.76 and 0.94 μg/m^3 at NJU and PAES, respectively, approximately ~~double~~ twice of those in another three months. The concentrations contributed by industry were significantly enhanced in certain periods (e.g., January 20th, April 9th-11th, and July 15th-17th), and industrial emissions were expected to be an important reason for the overestimation in BC concentrations through CTM (see the model evaluation in Section 3.3). Table ~~S3~~ S5 in the supplement summarizes the monthly and annual mean BC contributions by sector. The annual contributions of industry at the two sites were close to each other (21.0% and 21.9% at NJU and PAES respectively). Contributions of residential sources and transportation were higher at PAES resulting from large population and heavy traffic in the urban area. Minor contribution of power generation to BC concentrations was found at both sites (the annual means were less than 1%), attributed to its very limited emissions. The total contributions from the four ~~emission~~ sectors were larger than 50% for all the months and sites except for January. We assumed that the ~~much~~ smaller contributions in January ~~may~~ resulted partly from the longer lifetime of BC~~C~~ ~~because of~~ due to less wet deposition in winter.~~,~~ Moreover, we conducted the cluster analysis of back trajectories of air masses arriving at NJU with Hybrid Single Particle Lagrangian Integrated Trajectory (HYSPLIT, version 4) model, and found that ~~less~~fewer air masses passed through the third modeling domain in January, as illustrated in Figure S6 in the supplement. The result thus implied more contribution from regional transport to the air quality at the site in winter compared to other seasons. We acknowledged that the multiple regression model was less effective on identifying the sources of BC in winter by constraining the emissions in southern Jiangsu city cluster alone.~~Given the prevailing northerly wind directions in January, regional transport from boundary conditions accounted for the majority of contribution at two sites, the same as the result in other studies (Jia et al., 2008; Li et al., 2015; Sun et al., 2014). It thus would bring more uncertainty when estimating the top-down emissions in the multiple regression model in January. The uncertainty would be discussed in Section 3.3.~~

批注 [zy3]: 全称？

Summarized in Table 1 are the scaling factors β_1-β_4 estimated from multiple regression model (Eq. (1)) by season, together with the statistical indicators including the values of t, Sig. (or p) and variance inflation factor (VIF). The values of t and Sig. indicate statistical significance with a threshold of 2 and 0.05, respectively. VIF is a test for multicollinearity and the model is reasonable ~~with~~ when VIF values in the table are much smaller than 10. Since the emissions from power generation were small and they contributed very little to ambient BC concentrations, inclusion of power generation component would not significantly improve the regression model. In this study, therefore, we assumed that the simulated BC concentrations from power generation were correct by setting β_1 at 1 and further subtracted them from the observations. Most statistical indicators in Table 1 met the criteria (t>2, Sig.<0.05, VIF<10) and the overall significance was 0.00 in four months, implying acceptable robustness of the multiple regression model. However, the results were not statistically significant indicated by t and ~~p~~ Sig. values for some months and sectors (e.g., industry in April and October and residential in April and July), implying that the constrained emissions for those months/sectors need to be cautiously analyzed.

By applying β_1-β_4 in Eq. (2), the top-down estimates of BC emissions (JS-posterior) were estimated and illustrated in Figure 2. The total BC emissions for southern Jiangsu city cluster were calculated at 13.4 Gg, 50% smaller than those of JS-prior. For the capital city of Jiangsu Province, Nanjing, Huang et al. (in preparation) conducted detailed analysis on the changes in operation activities and emission control technologies of individual sources based on annually updated official environmental statistics and pollution census. With the bottom-up approach, the annual BC emissions in the city were estimated to decrease by 60% from 2012 to 2015 as shown in Figure S7 in the supplement. The relative change in annual emissions (60%) was close to that between JS-prior and JS-posterior (50%), implying the constraining approach in this work could capture the changes in emissions due to improved control measures.~~ and the validity of the two methods (the bottom-up approach by Huang et al. and the top-down approach in this work) could be verified.~~

The scaling factors of emissions from industry and transportation (β_2 and β_4) ranged from 0.22 to 0.42 and from 0.55 to 0.79 for different months, respectively. Accordingly, the emissions from industry and transportation in JS-posterior were estimated 67% and 32% smaller than those in JS-prior, respectively. As mentioned above, the emissions in JS-prior 2015 were simply scaled from those in 2012 according to activity data, and changes in emission factors were not considered. In the actual fact, however, a series of measures in industry and transportation were conducted to improve energy efficiency and to reduce emissions over recent years. Issued in 2013, for example, the Air Pollution Control Planning for the Key Regions for the 12th Five-Year Plan period (2010-2015) aimed to achieve 7% and 15% reductions in the annual average concentration and industrial emissions of fine particles in Jiangsu province from 2010 to 2015, respectively (Qian, 2013). The measures included eliminating old and energy-inefficient plants of heavy-polluted industries (thermal power generation and steel/building material production), and optimizing the energy structure through application of sustainable energy. Meanwhile, the enhanced use of cleaner gasoline and diesel products (National stage V standard) in transportation could lead to reduced vehicle emissions. The government efforts in emissions controls proved effective, indicated by the scaling factors much smaller than 1 (β_2 and β_4 in Table 1) and the reduced emissions of JS-posterior. For residential sources, the emissions in JS-posterior were 3% smaller than those in JS-prior, indicating limited difference in the annual total emissions between the two inventories. However, the scaling factors (β_3) in January and October were 1.31 and 1.52 respectively, showing a stronger enhancement in BC emissions in winter and autumn in JS-posterior than those in JS-prior. It thus implied that there were missing sources likely associated with low-quality fossil fuels or biofuel used for heating in winter and crop waste burning in autumn in JS-prior. ~~For the capital city of Jiangsu Province, Nanjing, Huang et al. (in preparation) conducted detailed analysis on the changes in operation activities and emission control technologies of individual sources based on annually updated official environmental statistics and pollution census. With the bottom-up approach, the annual BC emissions in the city were estimated to decrease by 60% from 2012 to 2015 as shown in Figure S6 in the supplement. The relative change in annual emissions was close to that between JS-prior and JS-posterior, and~~

~~the validity of the two methods (the bottom-up approach by Huang et al. and the top-down approach in this work) could be verified.~~

带格式的

Figure S8~~3~~ in the supplement presents the seasonal variations in BC emissions of JS-prior, JS-posterior and MEIC-prior by sector, and stronger variations were generally found in JS-posterior. As shown in Figure ~~3A~~S8a, the largest difference among the three inventories existed in the residential sources, and the ratio of maximum to minimum monthly emissions was 4.33 in JS-posterior, close to that in MEIC-prior at 4.00 and nearly 4 times of that in JS-prior at 1.13. ~~The analogue ratio for industry was 2.05 in JS-posterior, nearly twice of those in JS-prior at 1.14 and MEIC-prior at 1.12. The smallest difference was found for transportation among the three inventories. Seasonal variations in total emissions were a combination of those by sector weighted by the contribution of each sector to total emissions.~~ The ratios of maximum to minimum monthly emissions were 1.13, 1.83 and 1.29 for JS-prior, JS-posterior and MEIC-prior, respectively (Figure ~~3B~~S8b). The value for JS-posterior was closer to 2.1 for an anthropogenic BC emission inventory in China by Lu et al. (2011) that considered enhanced use of fossil fuels for residential heating in winter in northern China. The comparison thus implied again that current bottom-up inventories might underestimate the emissions of residential solid fuel burning in winter in southern Jiangsu. As central household heating was not conducted in the area in winter, the official energy statistics on which bottom-up inventories were based may not fully capture the elevated fuel burning by disperse households. Spatial distribution of BC emissions in JS-posterior was illustrated in Figure S3 in the supplement. Compared to JS-prior, BC emissions from industry and transportation were greatly reduced in downtown regions in southern Jiangsu city cluster.

3.3 Evaluation of the top-down emission estimate

The simulated BC concentrations based on bottom-up (JS-prior) and top-down estimation in emissions (JS-posterior) were compared with observations to evaluate the two inventories, and the results were illustrated in Figures 3~~4~~ and 4~~5~~ for NJU and

PAES~~ sites~~, respectively. Statistical indicators including mean concentrations from simulations and observations, NMB and NME, as well as the regression correlation (R) were calculated to evaluate the modeling performance, as summarized in Table 2.

In general, CTM based on JS-prior reproduced well the temporal variations of the observed BC concentrations at the two sites. The highest and lowest concentrations were respectively simulated in winter and summer, consistent with observations with an exception at PAES where the observed monthly mean in January (2.80 μg/m^3) was lower than that in October (3.62 μg/m^3). The overestimation in January at PAES (especially in middle and late January, 16^{th}–26^{th}) ~~may~~ might result partly from the emission control policy implemented for the National Memorial Day of Nanjing Massacre Victims in December 13^{th} in 2014. During the period, Nanjing was undertaking series of stringent restrictions on air pollutant emissions. For example, key petrochemical and steel industries were shut down, and all the high-pollution vehicles were forbidden to drive into the city~~ Nanjing~~. Those restrictions had large impacts on emissions and thereby air quality in the following month at PAES, but ~~have not~~were ~~been~~ not fully considered in current emission inventories. Moreover, the bias could be enhanced under certain meteorology conditions. ~~Meanwhile,~~As illustrated in Figure S~~8~~9 in the supplement, higher daily average PBL height at PAES was found for periods when the simulated concentrations were relatively lower (e.g., 6^{th} -7^{th}, 12^{th}-15^{th} and 28^{th}-31^{st}), resulting in smaller bias between simulation and observation. ~~we evaluated the effect of meteorology on the modeling performance at PAES, and the simulated daily average PBL heights at PAES were illustrated in Figure S8 in the supplement. For periods when simulated concentrations were lower than other period (e.g., 6^{th}–7^{th}, 12^{th}-15^{th} and 28^{th}-31^{st}), the simulated PBL height were higher so that it would help BC to disperse, resulting in lower simulations and smaller bias between simulations and observations.~~ In contrast, the lower PBL height found in other periods would exaggerate the overestimation in simulated concentrations, given the elevated

带格式的：上标

批注 [zy4]: check
明确到底是什么原因导致了模拟的偏差

emissions ~~the lower PBL heights in other periods would result in higher simulated concentrations and larger bias, let alone the overestimated emissions~~ in JS-prior. The seasonal variation of BC concentrations at NJU was larger than that at PAES, suggesting bigger impact of household solid fuel use on the suburban and rural regions. Though the model was able to capture the seasonal variability, discrepancies between simulations and observations existed, and CTM ~~commonly~~ generally underestimated BC concentrations at the suburban site NJU and overestimated those at the urban site PAES. With the monthly means ranged 1.99-5.97 μg/m^3 at NJU, the annual average ~~of~~ BC concentration (calculated as the mean of January, April, July and October) was simulated at 3.44 μg/m^3, smaller than the observed 3.83 μg/m^3. With the monthly means ranged 2.61-6.46 μg/m^3, in contrast, the annual concentration at PAES was simulated at 3.39 μg/m^3, larger than the observed 2.48 μg/m^3. Better correlation between observation and simulation was found at NJU, indicated by the larger R. The annual mean NMBs were calculated at -10.16% and 36.67%, and the NMEs were 41.15% and 72.00% at NJU and PAES, respectively. The discrepancy suggested that JS-prior used in CTM might misrepresent the spatial pattern of emissions. Population and economy densities were applied to allocate BC emissions, leading to overestimation in emissions and thereby simulated concentrations in urban areas with more population and economic activity. Besides, the model overestimated the peak surface concentrations at both sites particularly when the contribution from industry sector was enhanced as mentioned in Section 3.2 (e.g., January 9th-11th and April 9th-10th at NJU, and April 9th-12th, the second half of July, and October 20th at PAES).

Application of JS-posterior in CTM effectively corrected large biases between simulations and observations at the two sites. As shown in Table 2, NMEs were reduced for most months (all months at PAES and January and April at NJU) while effects of applying JS-posterior in CTM varied at two sites. At PAES, the annual average NME declined from 72.00% to 57.55% and the annual mean of BC concentration was simulated at 2.57 μg/m^3, in better agreement with the observed 2.48 μg/m^3 than the simulated 3.39 μg/m^3 using JS-prior. The largest reductions in NMEs were found in April and July, from 73.18% to 42.87% and from 92.74% to 42.37%, respectively. Moreover the overestimations in peak concentrations using JS-prior were partly corrected when JS-posterior was applied, resulting mainly from the reduced emissions from industry and transportation. Regarding the overestimation~~s~~ in January 16th-26th discussed above, we excluded the data points ~~during~~for those dates~~ese periods~~ and re-compared the observation~~s~~ and simulation. As can be seen ~~s, as shown~~ in Table S6 in the supplement, ~~. t~~The overestimation in CTM was largely reduced ~~when data were excluded~~ and the top-down estimate corrected the bias moderately in January at PAES. Besides the emissions, overestimation in~~Even after top-down constraint, simulated~~ annual BC concentration~~s~~ at PAES could ~~were~~result partly from the uncertainty in PBL modeling (Liu et al., 2018)~~ somewhat overestimated at PAES~~. As shown in Table S7 in the supplement, ~~We evaluated~~ the monthly PBL heights ~~height~~ in WRF ~~-model a~~~~were~~were~~t two sites~~ generally ~~in four months and found~~ lower ~~PBL height~~ than ~~the~~th~~at~~ose in actual atmosphere~~, as shown in Table S7 in the supplement. It could~~ , leading to~~result in~~ ~~the overestimation~~enhanced~~ of~~ BC concentrations~~ to some extent, the same result as in Liu et al. (2018).~~

Although simulations of peak concentrations at NJU were improved as well, the annual average NME at NJU slightly increased from 41.15% to 44.16% and the annual mean of BC concentration was simulated at 2.82 μg/m^3, smaller than the simulated 3.44 μg/m^3 using JS-prior. Bigger bias was found in July and October at NJU, since the reduced emission estimates in JS-posterior led to further underestimation in simulated ambient BC levels compared to JS-prior. Limitation of current multiple regression model was thus indicated that overestimation and underestimation in concentrations at different sites could hardly be corrected simultaneously without further improvement in spatial distribution of emissions.~~ For~~

~~the uncertainty in January due to the major contributions from boundary conditions, considering the relatively small bias between simulations and observations at NJU and PAES (excluding data in the middle and late January in Table S6 in the supplement) in JS-prior compared with other months, and the improvement of modeling performance in JS-posterior at two sites, as shown in Table 2, it implied the benefit of the top-down method even large uncertainty occurred in January.~~

4 Discussions

We selected April to evaluate the sensitivity of observation and bottom-up emission input to top-down constraint. Observation site number, spatial representativeness of sites, and the a ~~initial~~ priori bottom-up inventory were changed separately in the constraining approach, and various top-down estimates could be derived and compared with each other. ~~The statistical indicators of modeling performances based on different bottom-up and top-down emission estimates in April are summarized in Table 3.~~ Furthermore, we evaluated the uncertainty of the multiple regression model, including the assumption of near linearity between emissions and concentrations in July and October and the impact of precipitation in July. The statistical indicators of modeling performances based on different cases are summarized in Table 3. Details were described as below.

4.1 The effect of observation ~~site~~ data application ~~number~~

A major challenge in understanding the sources and distributions of BC in China was lack of a consistent and stable measurement network with good spatiotemporal coverage, such as the IMPROVE network in the United States (Malm et al., 1994). Uncertainty existed in the top-down estimates in this work, as hourly measurements on BC concentrations were only available at two sites in southern Jiangsu. Therefore, besides JS-posterior derived from observations at both sites in April as described in Section 3.2 (mentioned as Case 1 hereinafter), we conducted a Case 2 in which observation data at only one site (NJU) ~~was~~ were used in the top-down approach, to analyze the effect of the site number on emission estimates.

The scaling factors of emissions from industry, residential sources and transportation were recalculated at 0.42, 0.95 and 0.65, respectively. Compared ~~with~~ to ~~Scenario B~~JS-prior in April in Table 2, the NMEs of Case 2~~, as shown~~ in Table 3 ~~,~~ decreased from 42.31% to 32.47% and from 73.18% to 61.59% at NJU and PAES, respectively, implying the benefits of ground measurements (even available only at one site) on emission constraint. The NME in Case 2 was slightly smaller than that in Case 1 at NJU, suggesting that application of measurement data at one single site could improve modeling performance moderately at that site. At PAES, in contrast, much larger NME was found in Case 2. Much better modeling performance in Case 1 at PAES indicated that inclusion of more measurements with better spatiotemporal coverage could constrain BC emissions at city cluster level more effectively. ~~Regarding the averaged simulations and observations for all periods in Scenario B and Case 2, it seemed that top-down estimate magnified the discrepancy. Actually, It~~ should be noted that~~after the data screening mentioned in Section 2.2,~~ the number of data ~~applied~~ included in the multiple regression model was 48% of those~~ data~~ for~~ in~~ the whole~~all~~ period~~s (most data screening was due to lack of observations, accounting for 38%)~~ with the data screening mentioned in Section 2.2. In particular, –the period lack of observation accounted for 38% of the whole month. We ~~divided~~further analyzed the CTM performances for the~~ all the data points into two groups:~~ periods ~~those~~ included in the model and those excluded from the model separately, ~~and analyzed the modeling performances for both groups independently~~as shown in Table S8 in the supplement. The– observed concentration for the periods included in the model (2.56 μg/m^3)~~simulated concentration for periods included in the multiple regression model (2.71 μg/m^3)~~ was~~ larger~~ smaller than the ~~t~~simulated ~~he observation (2.56 μg/m^3)~~ in JS-prior (2.71 μg/m^3), ~~different from the case without data screening (i.e., data in all periods were included).~~leading to the reduced ~~–The~~ emissions~~ could~~

带格式的: 上标

带格式的: 上标

~~then be reduced~~ ~~when~~through constraining. ~~the observation was applied in the constraining. As a result, the~~ The constrained emissions resulted in a simulated ~~average~~ concentration ~~in Case 2 (2.42 μg/m³)~~ (2.42 μg/m^3 ~~in Table S8~~) ~~was~~ closer to the observation~~. At~~ for the periods included in the multiple regression model ~~the same time~~, and ~~the constrained emissions~~ did not increase the bias for the periods excluded from the ~~multiple regression~~ model. It ~~thus~~ ~~indicated~~suggested that factors other than emissions in CTM (e.g., meteorology) might contribute to ~~that~~ the ~~underestimation~~ underestimation –for ~~those~~the ~~periods~~latter. ~~, could result largely from factors other than emissions like meteorology.~~

~~4.2 The effect of spatial representativeness of observation sites~~

Besides the number of observation site, s~~S~~patial representativeness ~~of observation sites~~ was also identified and its impact on top-down emission constraint was evaluated. Considering the prevailing winds from northeast and southeast, on one hand, NJU located upwind Nanjing is hardly influenced by the emissions from the downtown of the city. Besides the site is downwind of ~~the Yangtze River Delta region (~~YRD~~)~~ including the Suzhou–Wuxi–Changzhou-Zhenjiang city cluster (Chen et al., 2017), thus it is more representative for the western YRD emissions through regional transport. On the other hand, PAES is located at urban Nanjing and its air quality is commonly influenced by surrounding transportation, residential, and commercial sources, thus the site is representative for the local emissions of Nanjing. In contrast to previous top-down studies that did not distinguish influence of local emissions and transport on air quality in sub-regions of the research domain (Wang et al., 2011; Fu et al., 2012), the spatial representativeness of the two observation sites were taken into account to improve the top-down approach and the result of constraining BC emissions in southern Jiangsu city cluster. Through the brute-force method described in Section 2.3, we zeroed out the emissions from Nanjing and Suzhou–Wuxi–Changzhou-Zhenjiang city cluster in CTM, respectively, and compared the simulated concentrations with those in Scenario B to analyze the contributions of the two regions to ambient BC concentrations at NJU and PAES ~~sites~~. As shown in Figure S10~~7~~ in the supplement, the contribution of emissions from Nanjing to PAES was greater than that to NJU in 82% of the modeling period, and the analogue number was 81% for the contribution of Suzhou–Wuxi–Changzhou-Zhenjiang city cluster to NJU greater than that to PAES. We thus concluded that emissions from Nanjing contributed significantly to PAES while those from Suzhou–Wuxi–Changzhou-Zhenjiang city cluster contributed significantly to NJU. We then developed a new case of top-down emission estimate in southern Jiangsu (Case 3), in which observation data at PAES and NJU were applied to constrain emissions from Nanjing and Suzhou–Wuxi–Changzhou-Zhenjiang city cluster, respectively.

The scaling factors in Case 3 are provided in Table 4. To avoid the collinearity in the multiple regression model, we expected that the relative changes in emissions from transportation in Nanjing and Suzhou–Wuxi–Changzhou-Zhenjiang city cluster were similar for recent years, resulting from the same progress of emission standard implementation (National Standard Stage IV) in southern Jiangsu and the frequent circulation of vehicles among the cities. Therefore a same scaling factor was assumed for transportation in the two regions. As shown in Table 4, all the scaling factors at PAES were smaller than those at NJU, implying that implementation of emission controls in Nanjing were more stringent than that in Suzhou–Wuxi–Changzhou-Zhenjiang city cluster from 2012 to 2015. As the host city of the 2nd Asian Youth Games in 2013 and the 2nd Youth Olympic Games in 2014, Nanjing was undertaking series of restrictions on air pollutant emissions. The city conducted emission control action on small coal-fired boilers since 2013 and over 1200 coal-fired boilers had been shut down by the end of 2014. In addition, central heating units were largely applied to replace the coal with electricity, natural gas or biofuel. As shown in Table 3, the NMEs in Case 3 were the smallest at both sites among all the cases with an exception: the NME at NJU in Case 3 was 32.64%, slightly larger than that in Case 2 at 32.47%. The result implied that inclusion of more measurement data with their spatial representativeness considered could improve the top-down approach in terms of spatial distribution of emissions and could reduce the deviation between observations and simulations.

Summarized in Table ~~5~~ S9 in the supplement are BC emissions from Nanjing and Suzhou–Wuxi–Changzhou-Zhenjiang city cluster estimated in different cases. All the top-down estimates were approximately half of the bottom-up estimate and the estimate in Case 1 was the smallest among all the cases. The same scaling factors were generated and applied in Cases 2 and 3 to calculate BC emissions from Suzhou–Wuxi–Changzhou-Zhenjiang city cluster which accounted for 80% of the total emissions in southern Jiangsu, resulting in similar top-down emission estimates between the two cases.

4.~~3~~ 2 The effect of ~~initial~~the –a priori bottom-up emission input

Given the large uncertainty in JS-prior that was simply developed based on the changes of activity levels in recent years, we applied MEIC-prior as well to explore the effect of the ~~initial~~ a priori emission inventory on top-down BC constraints.

Figures 5~~6~~ and 6~~7~~a compare the total amount and spatial distribution of emissions between JS-prior and MEIC-prior in April for southern Jiangsu, respectively. The total BC emissions ~~of southern Jiangsu city cluster~~ in JS-prior were 21% lower than those in MEIC-prior. In JS-prior, as shown in Figure 6~~7~~a, the emissions from some industrial plants were extremely larger than those in MEIC-prior, while the emissions in urban areas were found smaller. Both inventories indicated extremely small contribution from power generation. BC emissions from industry sector were calculated at 1.34 Gg in JS-prior, 0.22 Gg smaller than MEIC-prior. Emissions from industry in MEIC-prior were calculated based on regional average of emission factors and allocated according to spatial distribution of GDP. The method would possibly result in underestimation in emissions from big industrial plants but overestimation in urban areas. Emissions from residential sources in JS-prior were close to those in MEIC-prior as similar methodology was applied for the sector in the two inventories. BC emissions from transportation in MEIC-prior (0.85 Gg) were twice of those in JS-prior (0.42 Gg) attributable probably to the application of different emission factors. For on-road transportation, the emission factors in JS-prior were calculated with CORPERT model (EEA, 2012; Zhou et al., 2017) while they were obtained from available domestic measurements in MEIC-prior.

Simulation Case 4 was determined using MEIC-prior in CTM. ~~As shown in Table 3, the hourly average of BC concentrations at NJU was simulated at 2.49 μg/m^3 for April 2015 in Case 4, close to 2.38 μg/m^3 simulated with JS-prior (Scenario B). At PAES, however, application of MEIC-prior in CTM resulted in much larger concentration than JS-prior (5.13 versus 2.98 μg/m^3), indicating again that MEIC-prior would overestimate the emissions in urban area.~~ Following the top-down approach described in Section 2.2, we developed Case 5, using MEIC-prior instead of JS-prior as the a ~~initial~~ priori input of emission data in CTM. The scaling factors of emissions from industry, residential sources and transportation were respectively calculated at 0.15, 1.30 and 0.25 through multiple regression model, and the top-down estimate in BC emissions (mentioned as MEIC-posterior hereafter) were calculated at 0.75 Gg in April 2015, close to 0.78 Gg in the JS-posterior (Figure 5~~6~~). The differences in the emissions from industry and transportation between JS-posterior and MEIC-posterior were 0.06 and 0.07 Gg, respectively, much smaller than those between JS-prior and MEIC-prior. Besides the total amount, differences in spatial distribution in industry plants and urban areas between the top-down estimates (JS-posterior and MEIC-posterior) were also significantly reduced compared to those between bottom-up estimates (JS-prior and MEIC-prior), as shown in Figure 6~~7~~b.

As shown in Table 3, the monthly average BC concentration at NJU in Case 4 was simulated at 2.49 μg/m^3 for April 2015, close to 2.38 μg/m^3 simulated with JS-prior in Table 2. At PAES, however, application of MEIC-prior in CTM resulted in much larger concentration than JS-prior (5.13 versus 2.98 μg/m^3), indicating again that MEIC-prior would overestimate the emissions in urban area. Figure ~~8~~ 7 illustrates the scatterplots of the simulated BC concentrations from bottom-up and top-down inventories at NJU (Figure ~~8a~~7a) and PAES (Figure ~~8b~~7b). Using two bottom-up inventories in CTM, bigger difference in simulated BC concentrations was found at PAES compared to that at NJU, indicated by the slope (1.10) closer to 1 at NJU in Figure ~~8a~~7a. The correlation coefficients (R^2) between simulated BC concentrations using JS-prior and MEIC-prior were 0.81 at NJU and 0.40 at PAES respectively. Using two top-down estimates, the difference between simulated concentrations at PAES was significantly reduced and the slope got much closer to 1 in Figure ~~8b~~7b. The correlation coefficients (R^2) were enhanced to 0.94 and 0.87 at NJU and PAES, respectively.

To summarize, similar results from top-down constraint approach could be obtained in emission level, spatial distribution, and CTM performance, even clear difference existed in the a ~~initial~~ priori bottom-up inventories. In other word, limited effect of the a ~~initial~~ priori emission input was evaluated on the top-down estimate from the multiple regression model.

4.~~4~~ 3 ~~Uncertainty analysis~~ Evaluation of the near-linearity assumption in the multiple regression model

As mentioned in Section 2.2, the assumption of near linearity between emissions and concentrations is a principle of the multiple regression model, given the weak chemistry reactivity of BC. The principle has been applied in previous studies to constrain BC emissions (Fu et al., 2012; Kondo et al., 2011; Wang et al., 2013; Park et al., 2003; Verma et al., 2017). In the actual fact, however, processes other than chemical reaction, e.g., precipitation or wet deposition, impact the linearity. Therefore, the near-linear assumption needs to be justified, and the uncertainty of the methodology could then be evaluated.

Sensitivity analysis was conducted to assess the rationality of brute-force method described in Section 2.3, in which emissions of given sector were zeroed out to determine their contribution to the ambient concentrations. As summarized in Table ~~S4~~ S10 in the supplement, we ~~first~~ calculated the ratio of simulated wet deposition to emissions by month for NJU, PAES and the whole southern Jiangsu city cluster with JS-prior ~~(Scenario B)~~ and JS-posterior ~~(Case 1)~~, respectively. July and October were identified as the months with the most and least impact from precipitation, suggested by the largest and smallest ratio, respectively. Two sensitivity simulations were then conducted for the selected two months, in which doubled and halved emissions (i.e., 200% and 50% of emissions in JS-prior, respectively) were used in CTM, and the simulated concentrations were then compared to those with JS-prior ~~(i.e., Scenario B)~~ at NJU and PAES, as shown in~~.~~ Figures S11~~9~~ and S12 in the supplement respectively.~~10 illustrate the linear correlations of the simulated concentrations in these two sensitivity cases and the base scenario (Scenario B) at NJU and PAES, respectively. As can be seen in all the panels, the fraction of change in simulated monthly average concentration ($F_{conc.}$) was close to that of emission change ($F_{emis.}$), i.e., the ratio of $F_{emis.}$ to $F_{conc.}$ was around 1.0, within a range of ±10%. Similar ratio of change in emissions (⊿E) to that in simulated average concentration (⊿C) was obtained for each month and site as well.~~ ~~The results thus~~It suggested that the impact of non-linearity between emissions and concentrations was limited, no matter the precipitation was strong or not. As the top-down constrained emissions (JS-posterior) were 50% smaller than the bottom-up estimates (JS-prior), the relative change was far beyond the uncertainty from non-linearity (±10%, as discussed in Figure S12 in the supplement), implying the improvement of the top-down approach on emission estimation.

Many studies have reported the difficulty in precipitation simulation with WRF (Annor et al., 2017; Liu et al., 2018; Yu et al., 2011; Yang et al., 2014; Kaewmesri, 2018). In this study, the observed ground precipitation at Lukou, Liyang and Shanghai stations (see Figure 1 for locations) was compared with the simulated one to evaluate the WRF performance for precipitation modeling. As shown in Figures ~~S8~~S13-16~~1~~ in

批注 [u5]: 关于非线性的分析我移到 supplement Figures S10 和 S11 图表说明下面。

the supplement, the model ~~could capture the dates of precipitation, but it~~ generally overestimated the amount. Similar results were found in previous studies that WRF overestimated precipitation at fine spatial resolution (Politi et al., 2018; Kotlarski et al., 2014; García-Díez et al., 2015). Improvement in physics parameterization schemes in WRF will help better understand~~ing~~ the wet deposition of BC through simulation. To further evaluate the effect of wet deposition on emission constraining, we conducted an extra Case 6, in which the data influenced by simulated wet deposition (i.e., the periods with simulated wet deposition at hourly basis) were excluded in the top-down approach. The new scaling factors β_1'-β_4' estimated from the multiple regression model were summarized in Table ~~6~~5. By applying β_1'-β_4' in Eq. (2), the top-down estimates of annual BC emissions in Case 6 were calculated at 13.7 Gg, and the emissions by sector and month were illustrated in Table ~~7~~6, together with the relative deviation (RD) compared to emissions in~~ Case 1(~~ JS-posterior~~)~~. The relative deviations of monthly total emissions between Case 6 and ~~Case 1~~JS-posterior were less than 5%, with an exception of July at 14%, and that for annual total was 2.6%. Larger relative deviations were found for given sources, e.g., residential in January and transportation in July. The deviations, therefore, were much smaller than that between the emissions in JS-prior and JS-posterior. We consequently applied CTM to evaluate the modeling performance with the emissions in Case 6 for July. Illustrated in Table 3~~8~~ were the simulated BC concentrations and the statistic indicators obtained through comparisons with observation at the two sites. As suggested by the NME and R values, little improvement on CTM performance was achieved with the emissions in Case 6, compared to those with JS-posterior~~Case 1~~ (Table 2). The impact of simulated wet deposition on the top-down approach was thus expected to be moderate in this work.

As the simulated wet deposition varied from the reality to some extent and the impact of precipitation along the transport was not excluded in Case 6, we selected July to conduct a Case 7, in which the data influenced by accumulative precipitation along the back trajectories at the two sites were excluded in the multiple regression model. The merged high-quality precipitation measured by the Tropical Rainfall Measuring Mission (TRMM) satellite instrument was adopted for wet deposition screening, with a temporal resolution of 3 h and a spatial resolution of 0.25°×0.25°. We used ~~the Hybrid Single Particle Lagrangian Integrated Trajectory (~~HYSPLIT (~~,~~ version 4.9) model (http://www.ready.noaa.gov) to calculate the 48 h back trajectories of the air masses arriving at NJU and PAES. The back trajectories were calculated every 3 hour for July with the simulated layer heights of 50, 100 and 500 m above the ground and the time step of 3 h (the same as the temporal resolution of TRMM). The hourly accumulative precipitation along the 48 h back trajectories at two sites were then calculated to determine the BC-CO data pairs influenced by precipitation, given the little effect of precipitation on CO. Figure ~~11~~ 8 illustrates the changes in the ⊿BC/⊿CO ratio observed at two sites for different accumulated precipitation intervals. At NJU, the ⊿BC/⊿CO ratio of air masses receiving less than 3 mm accumulated precipitation was significantly larger than that of air masses receiving more than 3 mm, and the analogue number was 5 mm at PAES. In Case 7, therefore, we excluded the BC-CO data pairs receiving more than 3 mm and 5 mm accumulated precipitation along their trajectories within the last 48 h at NJU and PAES, respectively, in the multiple regression model. It minimized the effect of wet deposition while retained sufficient data points for the statistical significance. Figure 9~~12~~ shows the simulated wet deposition in Case 6 and the accumulated precipitation in Case 7 for July to compare the data selection in the two cases. In Case 6, the number of data points were reduced to 65% of Case 1 after data screening, and over 500 samples at the two sites were available for the multiple regression model. In Case 7, only 31% of data points remained. The periods excluded in Case 7 contained those in Case 6, implying a stricter data screening to eliminate the effect of precipitation.

Table ~~9~~ 5 shows the scaling factors estimated from the multiple regression model in Case 7, and no big changes were found compared to the scaling factors for July in

Case 6~~ (Table 6)~~. Consequently, the emissions by sector and total emissions in Case 7 were close to those in Case 6 (Table ~~7~~6). The relative deviation of total emissions in July between Case 7 and ~~Case 1~~JS-posterior (RD in Table ~~9~~6) was 13%, and those for residential and transportation were larger. The influence of precipitation was again indicated ~~insignificant~~modest, as the deviation was much smaller than that between the estimates obtained from the bottom-up and top-down methods. Moreover, the CTM performance based on Case 7, indicated by NMB and NME, was found similar to that based on Case 6, implying the small effect of precipitation screening on simulation. Even excluding the influence of precipitation along the back trajectories, the Sig. for residential sources in Case 7 was still much larger than 0.05 (Table ~~9~~5), suggesting more efforts on quantification of emissions for this highly uncertain source category.

5 Conclusions

Monthly top-down estimates of BC emissions were derived from a multiple regression model that integrated CTM and hourly BC concentrations from two ground observation sites in southern Jiangsu city cluster. The annual emissions from top-down approach (JS-posterior) were estimated at 13.4 Gg for 2015, 50.3% smaller than those in bottom-up emission inventory that did not include the improved emission controls in recent years (JS-prior), implying the effectiveness of air pollution prevention measures on emission abatement. Application of JS-posterior in CTM reduced the deviations between simulations and observations at two ground sites effectively, especially at the urban site PAES. The increased bias at NJU in certain months reflected the limitation of the top-down estimate. To evaluate the effects of observation data on top-down estimate, two more cases in which observation data of only one site (NJU) and observation data at both sites with their spatial representativeness differentiated were applied to constrain the emissions, respectively. Best CTM performance was found for the third case, indicating that inclusion of more ground measurements with better spatiotemporal coverage in the city cluster would improve the understanding of spatial distributions of BC emissions. In addition, top-down estimates were derived from various bottom-up inventories, and the differences in emission amount, spatial distribution and CTM performance between the constrained emission estimates were significantly reduced compared to those between the bottom-up inventories. The results implied that changes in the a ~~initial~~ priori emission input in the regression model and CTM had limited effect on the top-down estimation. Finally, the assumption of near-linearity between emissions and concentrations was justified, and the influence of wet deposition on the estimated emissions was evaluated to be moderate. This work demonstrated that top-down approach based on ground observations and CTM could capture the fast changes in BC emissions attributed to tightened pollution control policy at a city cluster scale. To further reduce uncertainty of the approach and apply the method to other regions, more ground measurements with sufficient temporal resolution would be recommended. ~~at other regions in the city cluster. Data from other sources, such as aerosol optical depth from satellite observation, could also be included to improve the spatial and temporal distributions of emission estimates.~~

Acknowledgement

This work was sponsored by the Natural Science Foundation of China (91644220 and 41575142) and the National Key Research and Development Program of China (2017YFC0210106 and 2016YFC0201507), ~~Natural Science Foundation of China (91644220 and 41575142)~~. We would like to acknowledge Tong Dan from Tsinghua University for national emission data (MEIC).

References

Annor, T., Lamptey, B., Wagner, S., Oguntunde, P., Arnault, J., Heinzeller, D., and Kunstmann, H.: High-resolution long-term WRF climate simulations over Volta

Basin. Part 1: validation analysis for temperature and precipitation, Theoretical and Applied Climatology, 133, 829-849, 10.1007/s00704-017-2223-5, 2017.

Baker, K., Johnson, M., and King, S.: Meteorological modeling performance summary for application to $PM_{2.5}$/haze/ozone modeling projects, Lake Michigan Air Directors Consortium, Midwest Regional Planning Organization, Des Plaines, Illinois, USA, 57 pp., 2004.

Bond, T. C., Streets, D. G., Yarber, K. F., Nelson, S. M., Woo, J. H., and Klimont, Z.: A technology-based global inventory of black and organic carbon emissions from combustion, Journal of Geophysical Research-Atmospheres, 109, 10.1029/2003jd003697, 2004.

Bond, T. C., Doherty, S. J., Fahey, D. W., Forster, P. M., Berntsen, T., DeAngelo, B. J., Flanner, M. G., Ghan, S., Kaercher, B., Koch, D., Kinne, S., Kondo, Y., Quinn, P. K., Sarofim, M. C., Schultz, M. G., Schulz, M., Venkataraman, C., Zhang, H., Zhang, S., Bellouin, N., Guttikunda, S. K., Hopke, P. K., Jacobson, M. Z., Kaiser, J. W., Klimont, Z., Lohmann, U., Schwarz, J. P., Shindell, D., Storelvmo, T., Warren, S. G., and Zender, C. S.: Bounding the role of black carbon in the climate system: A scientific assessment, Journal of Geophysical Research-Atmospheres, 118, 5380-5552, 10.1002/jgrd.50171, 2013.

Cao, G., Zhang, X., and Zheng, F.: Inventory of black carbon and organic carbon emissions from China, Atmospheric Environment, 40, 6516-6527, 10.1016/j.atmosenv.2006.05.070, 2006.

Chen, D., Cui, H., Zhao, Y., Yin, L., Lu, Y., and Wang, Q.: A two-year study of carbonaceous aerosols in ambient PM2.5 at a regional background site for western Yangtze River Delta, China, Atmospheric Research, 183, 351-361, 10.1016/j.atmosres.2016.09.004, 2017.

Cohen, J. B., and Wang, C.: Estimating global black carbon emissions using a top-down Kalman Filter approach, Journal of Geophysical Research: Atmospheres, 119, 307-323, 10.1002/2013jd019912, 2014.

Dachs, J., and Eisenreich, S. J.: Adsorption onto aerosol soot carbon dominates gas-particle partitioning of polycyclic aromatic hydrocarbons, Environmental science & technology, 34, 3690-3697, 10.1021/es991201+, 2000.

EEA (European Environment Agency): COPERT 4-Computer Programme to Calculate Emissions from Road Transport, User Manual (Version 9.0), Copenhagen, Denmark, 2012.

Emery, C., Tai, E., and Yarwood, G.: Enhanced meteorological modeling and performance evaluation for two Texas ozone episodes, 2001.

Fu, T. M., Cao, J. J., Zhang, X. Y., Lee, S. C., Zhang, Q., Han, Y. M., Qu, W. J., Han, Z., Zhang, R., Wang, Y. X., Chen, D., and Henze, D. K.: Carbonaceous aerosols in China: top-down constraints on primary sources and estimation of secondary contribution, Atmospheric Chemistry and Physics, 12, 2725-2746, 10.5194/acp-12-2725-2012, 2012.

García-Díez, M., Fernández, J., and Vautard, R.: An RCM multi-physics ensemble over Europe: multi-variable evaluation to avoid error compensation, Clim. Dyn., 45, 3141-3156, 10.1007/s00382-015-2529-x, 2015.

Gilardoni, S., Vignati, E., and Wilson, J.: Using measurements for evaluation of black carbon modeling, Atmospheric Chemistry and Physics, 11, 439-455, 10.5194/acp-11-439-2011, 2011.

Guerrette, J. J., and Henze, D. K.: Four-dimensional variational inversion of black carbon emissions during ARCTAS-CARB with WRFDA-Chem, Atmospheric Chemistry and Physics, 17, 7605-7633, 10.5194/acp-17-7605-2017, 2017.

Hong, C., Zhang, Q., He, K., Guan, D., Li, M., Liu, F., and Zheng, B.: Variations of China's emission estimates: response to uncertainties in energy statistics, Atmospheric Chemistry and Physics, 17, 1227-1239, 10.5194/acp-17-1227-2017, 2017.

Hu, Z., Zhao, C., Huang, J., Leung, L. R., Qian, Y., Yu, H., Huang, L., and Kalashnikova, O. V.: Trans-Pacific transport and evolution of aerosols: evaluation of quasi-global WRF-Chem simulation with multiple observations, Geoscientific Model Development, 9, 1725-1746, 10.5194/gmd-9-1725-2016, 2016.

Huang, Y., Zhao, Y, Qiu, L., Xie, F., Zhang, J., Huang, X.: The impacts of emission control and meteorology variation on reduced ambient $PM_{2.5}$ concentrations for a typical industrial city in Yangtze River Delta, China (in preparation).

Jacobson, M. Z.: Strong radiative heating due to the mixing state of black carbon in atmospheric aerosols, Nature, 409, 695-697, 10.1038/35055518, 2001.

Kaewmesri, P.: The Performance of Microphysics Scheme in Wrf Model for Simulating Extreme Rainfall Events, International Journal of GEOMATE, 15, 10.21660/2018.51.59256, 2018.

Koch, D., Schulz, M., Kinne, S., McNaughton, C., Spackman, J. R., Balkanski, Y., Bauer, S., Berntsen, T., Bond, T. C., Boucher, O., Chin, M., Clarke, A., De Luca, N., Dentener, F., Diehl, T., Dubovik, O., Easter, R., Fahey, D. W., Feichter, J., Fillmore, D., Freitag, S., Ghan, S., Ginoux, P., Gong, S., Horowitz, L., Iversen, T., Kirkevag, A., Klimont, Z., Kondo, Y., Krol, M., Liu, X., Miller, R., Montanaro, V., Moteki, N., Myhre, G., Penner, J. E., Perlwitz, J., Pitari, G., Reddy, S., Sahu, L., Sakamoto, H., Schuster, G., Schwarz, J. P., Seland, O., Stier, P., Takegawa, N., Takemura, T., Textor, C., van Aardenne, J. A., and Zhao, Y.: Evaluation of black carbon estimations in global aerosol models, Atmospheric Chemistry and Physics, 9, 9001-9026, 10.5194/acp-9-9001-2009, 2009.

Kondo, Y., Oshima, N., Kajino, M., Mikami, R., Moteki, N., Takegawa, N., Verma, R. L., Kajii, Y., Kato, S., and Takami, A.: Emissions of black carbon in East Asia estimated from observations at a remote site in the East China Sea, Journal of Geophysical Research-Atmospheres, 116, 10.1029/2011jd015637, 2011.

Kotlarski, S., Keuler, K., Christensen, O. B., Colette, A., Déqué, M., Gobiet, A., Goergen, K., Jacob, D., Lüthi, D., van Meijgaard, E., Nikulin, G., Schär, C., Teichmann, C., Vautard, R., Warrach-Sagi, K., and Wulfmeyer, V.: Regional climate modeling on European scales: a joint standard evaluation of the EURO-CORDEX

RCM ensemble, Geoscientific Model Development, 7, 1297-1333, 10.5194/gmd-7-1297-2014, 2014.

Kurokawa, J., Ohara, T., Morikawa, T., Hanayama, S., Janssens-Maenhout, G., Fukui, T., Kawashima, K., and Akimoto, H.: Emissions of air pollutants and greenhouse gases over Asian regions during 2000-2008: Regional Emission inventory in ASia (REAS) version 2, Atmospheric Chemistry and Physics, 13, 11019-11058, 10.5194/acp-13-11019-2013, 2013.

Lei, Y., Zhang, Q., He, K. B., and Streets, D. G.: Primary anthropogenic aerosol emission trends for China, 1990-2005, Atmospheric Chemistry and Physics, 11, 931-954, 10.5194/acp-11-931-2011, 2011.

Li, L., Chen, C. H., Fu, J. S., Huang, C., Streets, D. G., Huang, H. Y., Zhang, G. F., Wang, Y. J., Jang, C. J., Wang, H. L., Chen, Y. R., and Fu, J. M.: Air quality and emissions in the Yangtze River Delta, China, Atmos. Chem. Phys., 11, 1621–1639, doi:10.5194/acp-11-1621-2011, 2011.

Li, N., Fu, T. M., Cao, J. J., Zheng, J. Y., He, Q. Y., Long, X., Zhao, Z. Z., Cao, N. Y., Fu, J. S., and Lam, Y. F.: Observationally-constrained carbonaceous aerosol source estimates for the Pearl River Delta area of China, Atmospheric Chemistry and Physics Discussions, 15, 33583-33629, 10.5194/acpd-15-33583-2015, 2015.

Li, N., He, Q., Tie, X., Cao, J., Liu, S., Wang, Q., Li, G., Huang, R., and Zhang, Q.: Quantifying sources of elemental carbon over the Guanzhong Basin of China: A consistent network of measurements and WRF-Chem modeling, Environmental pollution, 214, 86-93, 10.1016/j.envpol.2016.03.046, 2016.

Liu, D., Yang, B., Zhang, Y., Qian, Y., Huang, A., Zhou, Y., and Zhang, L.: Combined impacts of convection and microphysics parameterizations on the simulations of precipitation and cloud properties over Asia, Atmospheric Research, 212, 172-185, 10.1016/j.atmosres.2018.05.017, 2018.

Liu, M., Lin, J., Wang, Y., Sun, Y., Zheng, B., Shao, J., Chen, L., Zheng, Y., Chen, J., Fu, T.-M., Yan, Y., Zhang, Q., and Wu, Z.: Spatiotemporal variability of NO_2 and

带格式的：下标

$PM_{2.5}$ over Eastern China: observational and model analyses with a novel statistical method, Atmospheric Chemistry and Physics, 18, 12933-12952, 10.5194/acp-18-12933-2018, 2018.

Lu, Z., Zhang, Q., and Streets, D. G.: Sulfur dioxide and primary carbonaceous aerosol emissions in China and India, 1996-2010, Atmospheric Chemistry and Physics, 11, 9839-9864, 10.5194/acp-11-9839-2011, 2011.

Malm, W. C., Sisler, J. F., Huffman, D., Eldred, R. A., and Cahill, T. A.:Spatial and seasonal trends in particle concentration and optical extinction in the United States , Journal of Geophysical Research-Atmospheres, 99, 1347-1370, 10.1029/93jd02916, 1994.

Matsui, H., Koike, M., Kondo, Y., Oshima, N., Moteki, N., Kanaya, Y., Takami, A., and Irwin, M.: Seasonal variations of Asian black carbon outflow to the Pacific: Contribution from anthropogenic sources in China and biomass burning sources in Siberia and Southeast Asia, Journal of Geophysical Research-Atmospheres, 118, 9948-9967, 10.1002/jgrd.50702, 2013.

Ohara, T., Akimoto, H., Kurokawa, J., Horii, N., Yamaji, K., Yan, X., and Hayasaka, T.: An Asian emission inventory of anthropogenic emission sources for the period 1980-2020, Atmospheric Chemistry and Physics, 7, 4419-4444, 10.5194/acp-7-4419-2007, 2007.

Park, R. J.: Sources of carbonaceous aerosols over the United States and implications for natural visibility, Journal of Geophysical Research, 108, 10.1029/2002jd003190, 2003.

Politi, N., Nastos, P. T., Sfetsos, A., Vlachogiannis, D., and Dalezios, N. R.: Evaluation of the AWR-WRF model configuration at high resolution over the domain of Greece, Atmospheric Research, 208, 229-245, 10.1016/j.atmosres.2017.10.019, 2018.

Qian, W.: Air Pollution Control Planning for the Key Regions during the 12th Five-Year Plan period (2010-2015), China Environmental Protection Industry, 4-18,

带格式的: 下标

2013.

Qin, Y., and Xie, S. D.: Spatial and temporal variation of anthropogenic black carbon emissions in China for the period 1980-2009, Atmospheric Chemistry and Physics, 12, 4825-4841, 10.5194/acp-12-4825-2012, 2012.

Ramanathan, V., and Carmichael, G.: Global and regional climate changes due to black carbon, Nature Geoscience, 1, 221-227, 10.1038/ngeo156, 2008.

Streets, D. G., Gupta, S., Waldhoff, S. T., Wang, M. Q., Bond, T. C., and Bo, Y. Y.: Black carbon emissions in China, Atmospheric Environment, 35, 4281-4296, 10.1016/s1352-2310(01)00179-0, 2001.

Streets, D. G., Bond, T. C., Carmichael, G. R., Fernandes, S. D., Fu, Q., He, D., Klimont, Z., Nelson, S. M., Tsai, N. Y., Wang, M. Q., Woo, J. H., and Yarber, K. F.: An inventory of gaseous and primary aerosol emissions in Asia in the year 2000, Journal of Geophysical Research-Atmospheres, 108, 10.1029/2002jd003093, 2003.

Verma, S., Reddy, D. M., Ghosh, S., Kumar, D. B., and Chowdhury, A. K.: Estimates of spatially and temporally resolved constrained black carbon emission over the Indian region using a strategic integrated modelling approach, Atmospheric Research, 195, 9-19, 10.1016/j.atmosres.2017.05.007, 2017.

Wang, Y., Wang, X., Kondo, Y., Kajino, M., Munger, J. W., and Hao, J.: Black carbon and its correlation with trace gases at a rural site in Beijing: Top-down constraints from ambient measurements on bottom-up emissions, Journal of Geophysical Research-Atmospheres, 116, 10.1029/2011jd016575, 2011.

Wang, X., Wang, Y., Hao, J., Kondo, Y., Irwin, M., Munger, J. W., and Zhao, Y.: Top-down estimate of China's black carbon emissions using surface observations: Sensitivity to observation representativeness and transport model error, Journal of Geophysical Research-Atmospheres, 118, 5781-5795, 10.1002/jgrd.50397, 2013.

Xia, Y., Zhao, Y., and Nielsen, C. P.: Benefits of of China's efforts in gaseous pollutant control indicated by the bottom-up emissions and satellite observations 2000-2014, Atmospheric Environment, 136, 43-53, 10.1016/j.atmosenv.2016.04.013, 2016.

Xu, X., Wang, J., Henze, D. K., Qu, W., and Kopacz, M.: Constraints on aerosol sources using GEOS-Chem adjoint and MODIS radiances, and evaluation with multisensor (OMI, MISR) data, Journal of Geophysical Research-Atmospheres, 118, 10139-10139, 10.1002/jgrd.50784, 2013.

Yang, B., Zhang, Y., Qian, Y., Huang, A., and Yan, H.: Calibration of a convective parameterization scheme in the WRF model and its impact on the simulation of East Asian summer monsoon precipitation, Clim. Dyn., 44, 1661-1684, 10.1007/s00382-014-2118-4, 2014.

Yu, E., Wang, H., Gao, Y., and Sun, J.: Impacts of cumulus convective parameterization schemes on summer monsoon precipitation simulation over China, Acta Meteorologica Sinica, 25, 581-592, 10.1007/s13351-011-0504-y, 2011.

Zhang, L., Henze, D. K., Grell, G. A., Carmichael, G. R., Bousserez, N., Zhang, Q., Torres, O., Ahn, C., Lu, Z., Cao, J., and Mao, Y.: Constraining black carbon aerosol over Asia using OMI aerosol absorption optical depth and the adjoint of GEOS-Chem, Atmospheric Chemistry and Physics, 15, 10281-10308, 10.5194/acp-15-10281-2015, 2015.

Zhang, Q., Streets, D. G., Carmichael, G. R., He, K. B., Huo, H., Kannari, A., Klimont, Z., Park, I. S., Reddy, S., Fu, J. S., Chen, D., Duan, L., Lei, Y., Wang, L. T., and Yao, Z. L.: Asian emissions in 2006 for the NASA INTEX-B mission, Atmospheric Chemistry and Physics, 9, 5131-5153, 10.5194/acp-9-5131-2009, 2009.

Zhang, Y., Liu, P., Pun, B., and Seigneur, C.: A comprehensive performance evaluation of MM5-CMAQ for the Summer 1999 Southern Oxidants Study episode - Part I: Evaluation protocols, databases, and meteorological predictions, Atmospheric Environment, 40, 4825-4838, 10.1016/j.atmosenv.2005.12.043, 2006.

Zhao, Y., Zhang, J., and Nielsen, C. P.: The effects of energy paths and emission controls and standards on future trends in China’s emissions of primary air pollutants, Atmospheric Chemistry and Physics, 14, 8849-8868, doi:10.5194/acp-14-8849-2014, 2014.

Zhao, Y., Zhang, J., and Nielsen, C. P.: The effects of recent control policies on trends in emissions of anthropogenic atmospheric pollutants and CO_2 in China, Atmospheric Chemistry and Physics, 13, 487-508, 10.5194/acp-13-487-2013, 2013.

Zheng, J., He, M., Shen, X., Yin, S., and Yuan, Z.: High resolution of black carbon and organic carbon emissions in the Pearl River Delta region, China, Science of the Total Environment, 438, 189-200, 10.1016/j.scitotenv.2012.08.068, 2012.

Zhou, Y., Zhao, Y., Mao, P., Zhang, Q., Zhang, J., Qiu, L., and Yang, Y.: Development of a high-resolution emission inventory and its evaluation and application through air quality modeling for Jiangsu Province, China, Atmospheric Chemistry and Physics, 17, 211-233, 10.5194/acp-17-211-2017, 2017.

Figure captions

Figure 1. Modeling domain and locations of two observation sites and ~~three~~ four meteorological stations.

Figure 2. The monthly (left axis) and annual emissions (right axis) by sector for southern Jiangsu 2015 in JS-prior and JS-posterior (unit: Gg).

~~Figure 3. The seasonal variation of BC emissions by source (a) and total emissions (b) in JS-prior, JS-posterior and MEIC-prior.~~

Figure 3~~4~~. The observed and simulated hourly BC concentrations at NJU using JS-prior and JS-posterior for January (a), April (b), July (c) and October (d) in 2015 (unit: ug/m^3).

Figure 4~~5~~. The same as Figure ~~4~~ 3 but at PAES (unit: ug/m^3).

Figure 5~~6~~. BC emission estimates by source of JS-prior, MEIC-prior, JS-posterior, and MEIC-posterior in April 2015 in southern Jiangsu (unit: Gg).

Figure 6~~7~~. The spatial distributions of the deviations (JS-MEIC, unit: Mg) between JS-prior and MEIC-prior (a) and those between JS-posterior and MEIC-posterior (b).

Figure 7~~8~~. The scatter plots of the simulated BC concentrations using JS inventories versus those using MEIC at NJU (a) and PAES (b).

~~Figure 9. The correlation between the simulated BC concentrations with JS-prior and those with doubled (a and c) or halved emissions in JS-prior (b and d) in July (a and b) and October (c and d) at NJU.~~ ~~F_{emis} and F_{conc} indicate respectively the fraction of changed emissions and that of changed simulated monthly average concentrations between sensitivity and base simulation (Scenario B).~~ ~~ΔE and ΔC indicated the change in emissions and that in simulated monthly average concentrations, respectively.~~

~~Figure 10. The same as Figure 9 but at PAES.~~

Figure 8~~11~~. The⊿BC/⊿CO ratio at NJU (a) and PAES (b) separated by different accumulated precipitation along the back trajectories during 48 h. The data point number of ~~remaining data points~~each accumulated precipitation interval (right axis) is also given.

Figure 9~~12~~. The wet deposition in Case 6 (right axis, unit: kg/hectare) and accumulated precipitation~~–~~ in Case 7 (left axis, mm) at NJU (a) and PAES (b). The number of remaining data points is also given.

Tables

Table 1. The scaling factors and statistical indicators from the multiple regression model for estimation of JS-posterior.

Month	Sector	Scaling factor	t[a]	Sig.[b]	VIF[c]	Sig.[d]
	Industry (β_2)	0.42	2.65	0.01	1.76	
January	Residential (β_3)	1.31	3.67	0.00	2.37	0.00
	Transportation (β_4)	0.79	2.23	0.03	2.72	
	Industry (β_2)	0.22	0.96	0.34	2.65	
April	Residential (β_3)	0.58	1.63	0.11	4.62	0.00
	Transportation (β_4)	0.67	2.21	0.03	4.19	
	Industry (β_2)	0.35	3.09	0.00	2.09	
July	Residential (β_3)	0.39	0.95	0.34	2.95	0.00
	Transportation (β_4)	0.55	2.20	0.03	3.46	
	Industry (β_2)	0.34	1.92	0.06	1.53	
October	Residential (β_3)	1.52	4.12	0.00	2.20	0.00
	Transportation (β_4)	0.74	2.80	0.01	2.65	

Note: The criteria for the statistical significance of the model: a: t>2, b: Sig.<0.05, and c: VIF<10, d: the overall significance<0.05.

Table 2. Statistical indicators for observed and simulated BC concentrations using JS-prior and JS-posterior at NJU and PAES.

Site	Parameter	January		April		July		October		Annual	
		JS-prior	JS-posterior	JS-prior	JS-posterior	JS-prior	JS-posterior	JS-prior	JS-posterior	JS-prior	JS-posterior
NJU	Average SIM ($\mu g/m^3$)	5.97	5.50	2.38	1.82	1.99	1.29	2.80	2.42	3.44	2.82
	Average OBS ($\mu g/m^3$)	5.44	5.44	2.69	2.69	2.65	2.65	3.96	3.96	3.83	3.83
	NMB (%)	8.35	-0.08	-16.02	-32.40	-23.09	-51.32	-29.20	-39.01	-10.16	-26.43
	NME (%)	37.83	35.54	42.31	38.61	49.62	57.49	40.52	43.06	41.15	44.16
	R	0.67	0.66	0.34	0.43	0.36	0.31	0.42	0.48	0.67	0.69
PAES	Average SIM ($\mu g/m^3$)	6.46	5.91	2.98	1.95	2.61	1.63	3.19	2.88	3.39	2.57
	Average OBS ($\mu g/m^3$)	2.80	2.80	1.70	1.70	1.51	1.51	3.62	3.62	2.48	2.48
	NMB (%)	151.93	134.59	61.57	14.73	72.17	8.28	-12.01	-20.48	36.67	3.54
	NME (%)	155.53	139.50	73.18	42.87	92.74	42.37	43.10	40.80	72.00	57.55
	R	0.38	0.38	0.64	0.53	0.35	0.37	0.57	0.72	0.38	0.45

Note: SIM and OBS indicated the results from simulation and observation, respectively. NMB and NME were calculated using following equations (P and O indicated the results from modeling prediction and observation, respectively):

$$NMB = \frac{\sum_{i=1}^{n}(P_i - O_i)}{\sum_{i=1}^{n} O_i} \times 100\% ;\ .\ NME = \frac{\sum_{i=1}^{n}|P_i - O_i|}{\sum_{i=1}^{n} O_i} \times 100\%$$

Table 3. Statistical indicators for observed and simulated BC concentrations in different cases~~ in April 2015~~ at NJU and PAES (Cases 1-5 for April, and Cases 6-7 for July).

Site	Parameter	Case1	Case2	Case3	Case4	Case5	Case 6	Case 7
	Average SIM (μg/m^3)	1.82	2.27	2.06	2.49	1.78	1.40	1.41
	Average OBS (μg/m^3)	2.69	2.69	2.69	2.69	2.69	2.65	2.65
NJU	NMB (%)	-32.40	-21.59	-23.50	-7.46	-33.95	-47.41	-46.72
	NME (%)	38.61	32.47	32.64	41.58	38.94	54.88	54.44
	R	0.43	0.49	0.49	0.40	0.46	0.33	0.33
	Average SIM (μg/m^3)	1.95	2.45	2.01	5.13	2.29	1.76	1.76
	Average OBS (μg/m^3)	1.70	1.70	1.70	1.70	1.70	1.51	1.51
PAES	NMB (%)	14.73	49.86	18.02	201.35	34.71	16.87	16.65
	NME (%)	42.87	61.59	39.62	201.56	47.73	44.46	42.71
	R	0.53	0.63	0.66	0.65	0.59	0.36	0.39

Note:

Case 1 applied observations at two sites to constrain the emissions from the whole city cluster (JS-posterior); Case 2 applied observations at only one site (NJU) to constrain the whole city cluster; Case 3 applied observations at two sites to constrain emissions from different cities respectively; Case 4 applied the MEIC-prior; Case 5 applied the MEIC-posterior; Case 6 excluded the data influenced by simulated wet deposition; and Case 7 excluded the data influenced by satellite-derived accumulative precipitation.

带格式表格

带格式的：正文

~~Case 1: using observations at two sites to constrain whole city cluster (JS-posterior)~~
~~Case 2: using observations at only one site (NJU) to constrain whole city cluster~~
~~Case 3: using observations at two sites to constrain different cities respectively~~
~~Case 4: using MEIC-prior~~
~~Case 5: using MEIC-posterior~~
~~Case 6: excluding data influenced by simulated wet deposition~~
~~Case 7: excluding data influenced by satellite-derived accumulative precipitation.~~

带格式的: 正文

1176 **Table 4. The scaling factors and statistical indicators from the multiple**
1177 **regression model in Case 3.**

Site	Sector	Scaling factor	t	Sig.	VIF
NJU	Industry (β_2)	0.42	1.71	0.09	2.03
	Residential (β_3)	0.95	2.50	0.01	2.52
	Transportation (β_4)	0.65	2.13	0.03	2.66
PAES	Industry (β_2)	0.19	3.46	0.00	1.44
	Residential (β_3)	0.36	1.89	0.06	1.44
	Transportation(β_4)	0.65	-	-	-

~~Table 5. BC emissions from Nanjing and Suzhou–Wuxi–Changzhou-Zhenjiang city cluster in different cases in April 2015 (Gg).~~

带格式的：正文

~~Case~~	~~Sector~~	~~Nanjing~~	~~Suzhou–Wuxi–Changzhou–Zhenjiang~~	~~Southern Jiangsu~~
	~~Power~~	~~0~~	~~0.01~~	~~0.01~~
	~~Industry~~	~~0.21~~	~~1.13~~	~~1.34~~
~~Scenario B~~	~~Residential~~	~~0.08~~	~~0.24~~	~~0.32~~
	~~Transportation~~	~~0.12~~	~~0.30~~	~~0.42~~
	~~Total~~	~~0.41~~	~~1.68~~	~~2.09~~
	~~Power~~	~~0~~	~~0.01~~	~~0.01~~
	~~Industry~~	~~0.05~~	~~0.25~~	~~0.30~~
~~Case 1~~	~~Residential~~	~~0.04~~	~~0.14~~	~~0.19~~
	~~Transportation~~	~~0.08~~	~~0.20~~	~~0.28~~
	~~Total~~	~~0.17~~	~~0.60~~	~~0.78~~
	~~Power~~	~~0~~	~~0.01~~	~~0.01~~
	~~Industry~~	~~0.09~~	~~0.47~~	~~0.56~~
~~Case 2~~	~~Residential~~	~~0.07~~	~~0.23~~	~~0.30~~
	~~Transportation~~	~~0.08~~	~~0.20~~	~~0.27~~
	~~Total~~	~~0.24~~	~~0.91~~	~~1.14~~
	~~Power~~	~~0~~	~~0.01~~	~~0.01~~
	~~Industry~~	~~0.04~~	~~0.47~~	~~0.51~~
~~Case 3~~	~~Residential~~	~~0.03~~	~~0.23~~	~~0.26~~
	~~Transportation~~	~~0.08~~	~~0.20~~	~~0.27~~
	~~Total~~	~~0.15~~	~~0.90~~	~~1.05~~

Table 5. The scaling factors and statistical indicators from the multiple regression model in Cases 6 and 7.

~~Table 6. The scaling factors and statistical indicators from the multiple regression model in Case 6.~~

	Month	Sector	Scaling factor	t[a]	Sig.[b]	VIF[c]	Sig.[d]
Case 6	January	Industry (β_2')	0.41	2.17	0.03	1.71	0.00
		Residential (β_3')	1.53	3.48	0.00	2.29	
		Transportation (β_4')	0.73	1.65	0.10	2.66	
	April	Industry (β_2')	0.24	0.92	0.36	1.91	0.00
		Residential (β_3')	0.51	1.32	0.19	3.29	
		Transportation (β_4')	0.70	2.12	0.03	3.03	
	July	Industry (β_2')	0.38	4.43	0.00	1.43	0.00
		Residential (β_3')	0.34	0.82	0.41	2.52	
		Transportation (β_4')	0.74	3.55	0.00	2.25	
	October	Industry (β_2')	0.33	1.00	0.32	1.44	0.00
		Residential (β_3')	1.36	2.61	0.01	1.86	
		Transportation (β_4')	0.72	1.89	0.06	2.02	
Case 7	July	Industry (β_2')	0.38	2.38	0.02	1.31	0.00
		Residential (β_3')	0.31	0.31	0.75	2.31	
		Transportation (β_4')	0.75	1.8	0.07	1.95	

~~Note: The criteria for the statistical significance of the model: a: t>2, b: Sig.<0.05, and c: VIF<10, d: the overall significance.~~

带格式的：正文

带格式表格

带格式的：居中

Table ~~7~~6. The monthly and annual emissions by sector for southern Jiangsu 2015 in Cases 6 and 7 (unit: Gg) and the relative deviation compared to ~~Case 1~~JS-posterior (RD: Case 6 or 7–~~Case 1~~JS-posterior)/ JS-posterior, %~~Case 1~~).

	January		April		July		October		Annual		July	
	Case 6	RD	Case 6	RD	Case 6	RD	Case 6	RD	Case 6	RD	Case 7	RD
Power	0.0	0.0~~%~~	0.0	0.0~~%~~	0.0	0.0~~%~~	0.0	0.0~~%~~	0.0	0.0~~%~~	0.0	0.0
Industry	0.6	-2.4~~%~~	0.3	9.9~~%~~	0.6	9.2~~%~~	0.5	-0.3~~%~~	6.0	3.1~~%~~	0.5	9.5
Residential	0.5	16.7~~%~~	0.2	-13.1~~%~~	0.1	-13.7~~%~~	0.4	-10.2~~%~~	3.6	-0.6~~%~~	0.1	-20.6
Transportation	0.3	-8.2~~%~~	0.3	4.3~~%~~	0.4	34.4~~%~~	0.3	-3.0~~%~~	3.9	5.4~~%~~	0.4	36.4
Sum	1.4	2.4~~%~~	0.8	2.3~~%~~	1.1	13.6~~%~~	1.2	-4.2~~%~~	13.5	2.6~~%~~	1.0	13.4

带格式表格

~~Table 8. Statistical indicators for the observed and simulated BC concentrations in July 2015 at NJU and PAES in Case 6 and Case 7.~~

	Parameter	Case 6	Case 7
NJU	Average SIM (μg/m^3)	1.40	1.41
	Average OBS (μg/m^3)	2.65	2.65
	NMB (%)	-47.41	-46.72
	NME (%)	54.88	54.44
	R	0.33	0.33
PAES	Average SIM (μg/m^3)	1.76	1.76
	Average OBS (μg/m^3)	1.51	1.51
	NMB (%)	16.87	16.65
	NME (%)	44.46	42.71
	R	0.36	0.39

~~Note: SIM and OBS indicated the results from simulation and observation, respectively. NMB and NME were calculated using following equations (P and O indicated the results from modeling prediction and observation, respectively):~~

$$NMB = \frac{\sum_{i=1}^{n}(P_i - O_i)}{\sum_{i=1}^{n} O_i} \times 100\% \; ; \quad NME = \frac{\sum_{i=1}^{n}|P_i - O_i|}{\sum_{i=1}^{n} O_i} \times 100\%$$

~~Table 9. The scaling factors and statistical indicators from the multiple regression model in Case 7. The emissions by sector for southern Jiangsu 2015 July in Case 7 (unit: Gg) and the relative deviations (RD) compared to Case 1 (RD: Case 7–Case 1)/Case 1) are also shown in table.~~

~~Sector~~	~~Scaling factor~~	~~t~~[a]	~~Sig.~~[b]	~~VIF~~[c]	~~Sig.~~[d]	~~Emissions~~	~~RD~~
~~Power~~						~~0.0~~	~~0.0%~~
~~Industry (β_2')~~	~~0.38~~	~~2.38~~	~~0.02~~	~~1.31~~		~~0.5~~	~~9.5%~~
~~Residential (β_3')~~	~~0.31~~	~~0.31~~	~~0.75~~	~~2.31~~	~~0.00~~	~~0.1~~	~~-20.6%~~
~~Transportation (β_4')~~	~~0.75~~	~~1.8~~	~~0.07~~	~~1.95~~		~~0.4~~	~~36.4%~~
~~Sum~~						~~1.0~~	~~13.4%~~

~~Note: The criteria for the statistical significance of the model: a: t>2, b: Sig.<0.05, and c: VIF<10, d: the overall significance.~~

Figure 1

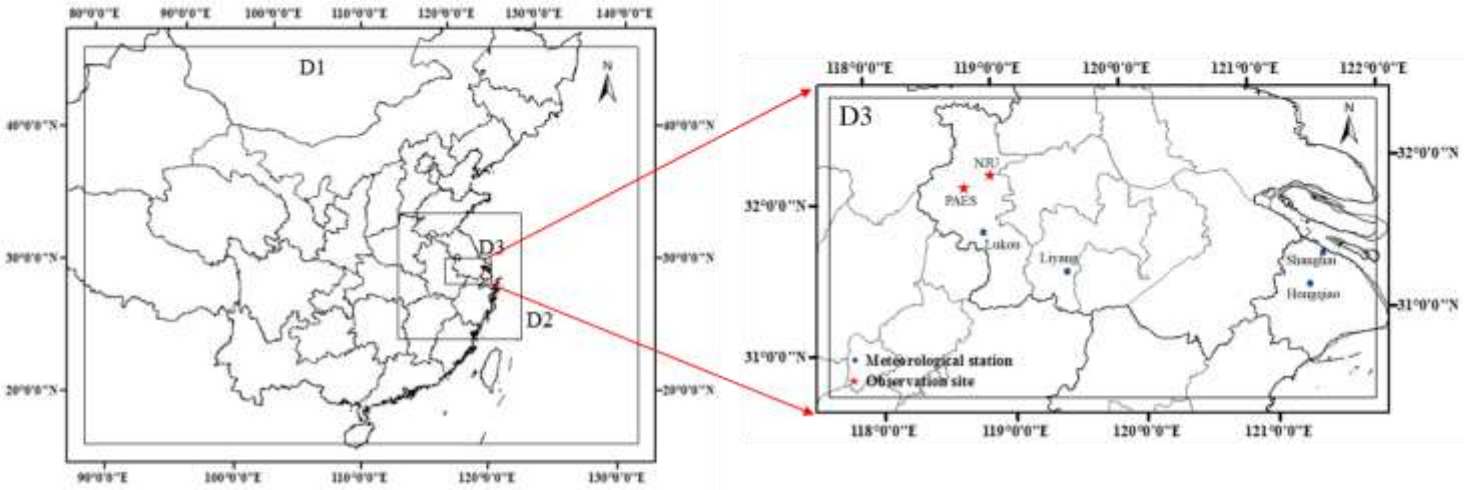
D1
D2
D3
N
D3
N
NRJ
PAES
Lukou
Liyang
Hongqiao
Meteorological station
Observation site
118°0'0"E
119°0'0"E
120°0'0"E
121°0'0"E
122°0'0"E
32°0'0"N
31°0'0"N

~~**Figure 2**~~

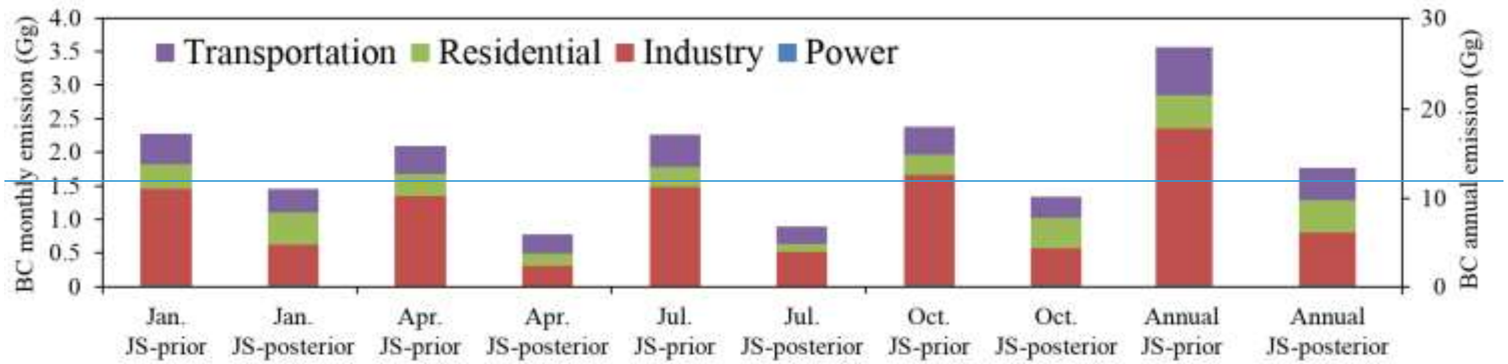

Transportation
Residential
Industry
Power
BC monthly emission (Gg)
BC annual emission (Gg)
4.0
3.5
3.0
2.5
2.0
1.5
1.0
0.5
0
30
20
10
0
Jan. JS-prior
Jan. JS-posterior
Apr. JS-prior
Apr. JS-posterior
Jul. JS-prior
Jul. JS-posterior
Oct. JS-prior
Oct. JS-posterior
Annual JS-prior
Annual JS-posterior

Figure 2

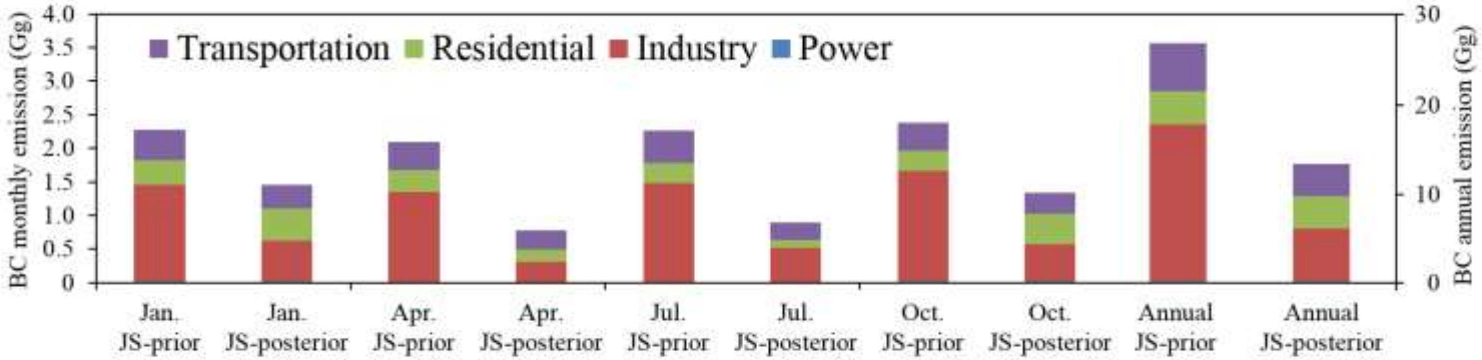

Transportation
Residential
Industry
Power
BC monthly emission (Gg)
BC annual emission (Gg)
4.0
3.5
3.0
2.5
2.0
1.5
1.0
0.5
0
30
20
10
0
Jan. JS-prior
Jan. JS-posterior
Apr. JS-prior
Apr. JS-posterior
Jul. JS-prior
Jul. JS-posterior
Oct. JS-prior
Oct. JS-posterior
Annual JS-prior
Annual JS-posterior

Figure 3~~**Figure 3**~~

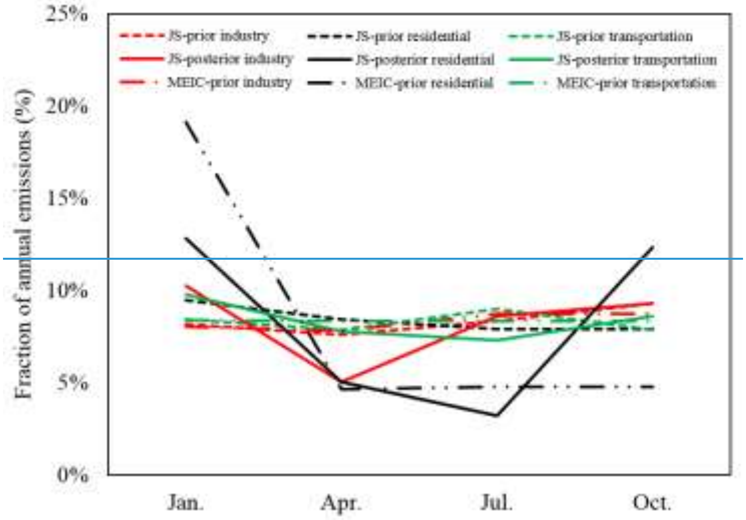

~~(a)~~

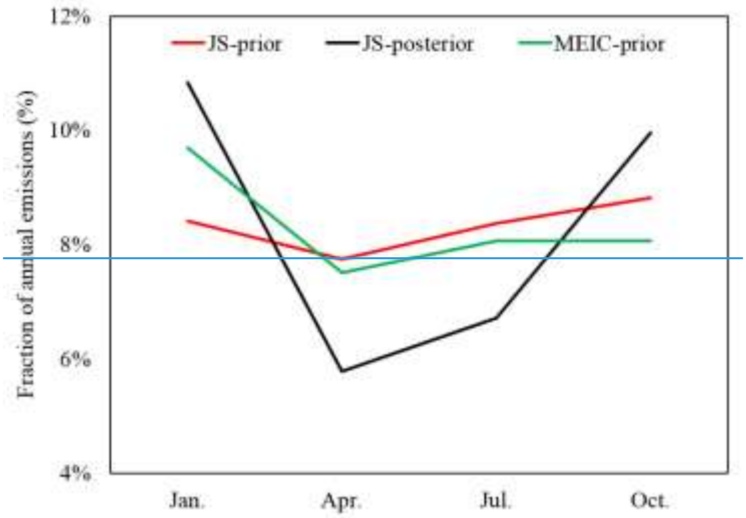

~~(b)~~

~~Figure 4~~

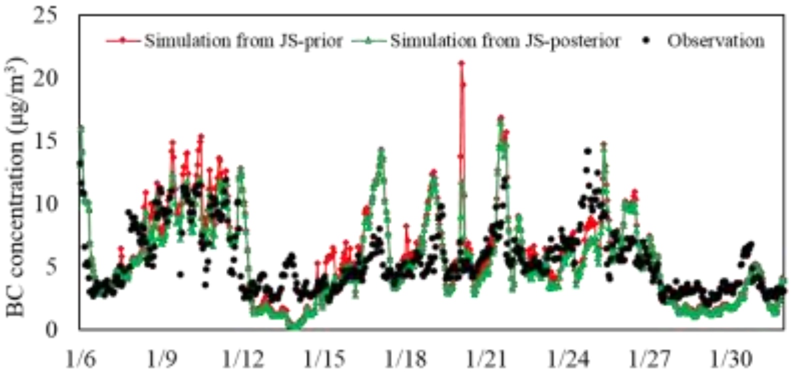

Simulation from JS-prior
Simulation from JS-posterior
Observation
BC concentration (μg/m³)
0
5
10
15
20
25
1/6
1/9
1/12
1/15
1/18
1/21
1/24
1/27
1/30

(a)

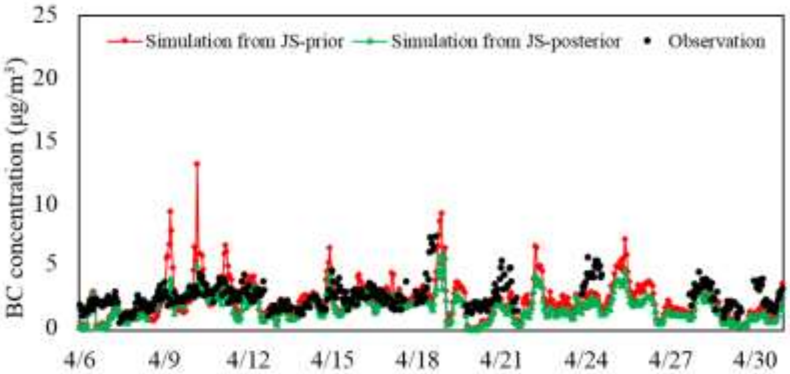

Simulation from JS-prior
Simulation from JS-posterior
Observation
BC concentration (μg/m³)
0
5
10
15
20
25
4/6
4/9
4/12
4/15
4/18
4/21
4/24
4/27
4/30

(b)

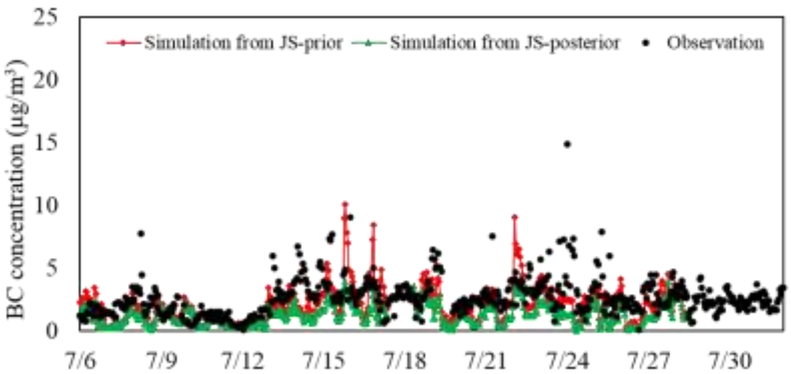

Simulation from JS-prior
Simulation from JS-posterior
Observation
BC concentration (μg/m³)
0
5
10
15
20
25
7/6
7/9
7/12
7/15
7/18
7/21
7/24
7/27
7/30

(c)

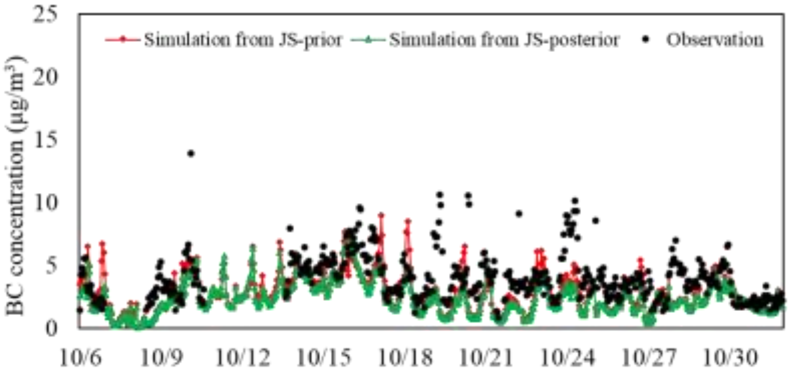

Simulation from JS-prior
Simulation from JS-posterior
Observation
BC concentration (μg/m³)
25
20
15
10
5
0
10/6
10/9
10/12
10/15
10/18
10/21
10/24
10/27
10/30

(d)

1250

Figure 4~~5~~

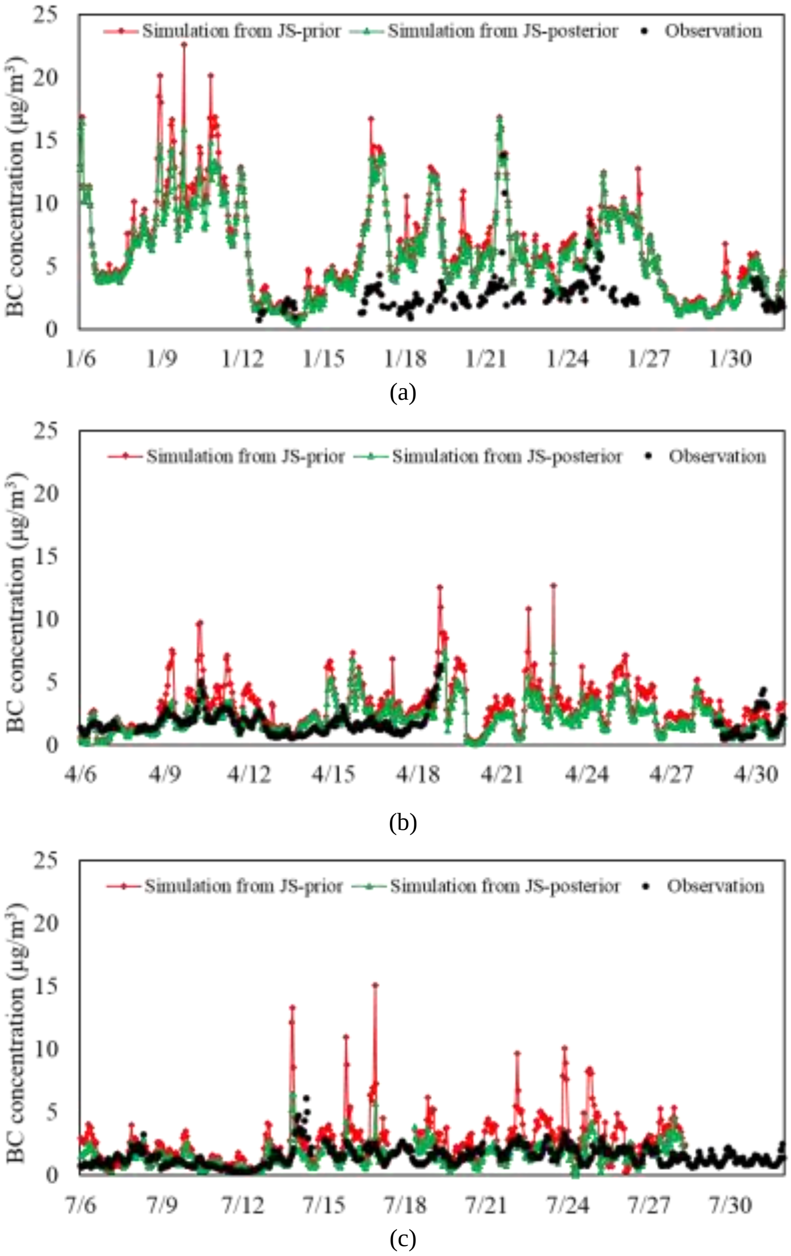
Simulation from JS-prior
Simulation from JS-posterior
Observation
BC concentration (μg/m³)
25
20
15
10
5
0
1/6
1/9
1/12
1/15
1/18
1/21
1/24
1/27
1/30
(a)
Simulation from JS-prior
Simulation from JS-posterior
Observation
BC concentration (μg/m³)
4/6
4/9
4/12
4/15
4/18
4/21
4/24
4/27
4/30
(b)
Simulation from JS-prior
Simulation from JS-posterior
Observation
BC concentration (μg/m³)
7/6
7/9
7/12
7/15
7/18
7/21
7/24
7/27
7/30
(c)

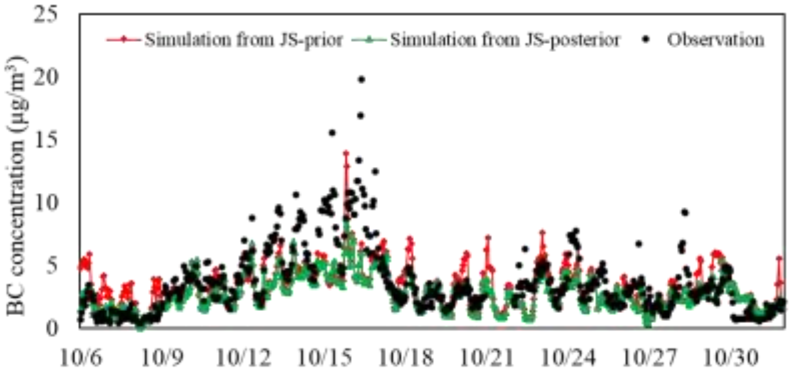
Simulation from JS-prior
Simulation from JS-posterior
Observation
BC concentration (μg/m³)
0
5
10
15
20
25
10/6
10/9
10/12
10/15
10/18
10/21
10/24
10/27
10/30

(d)

Figure 5~~6~~

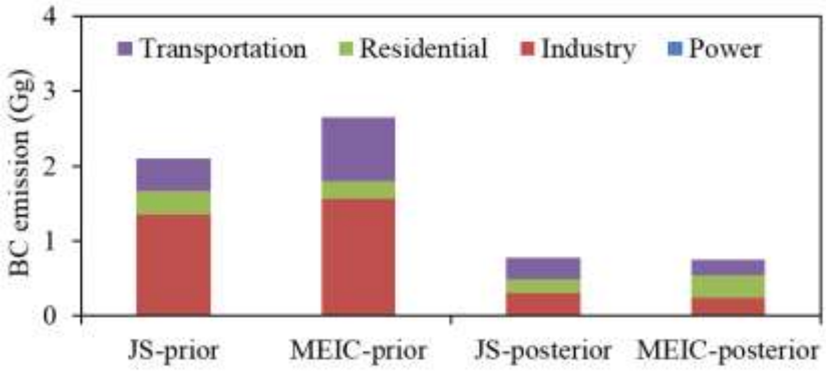

Transportation
Residential
Industry
Power
BC emission (Gg)
4
3
2
1
0
JS-prior
MEIC-prior
JS-posterior
MEIC-posterior

Figure 6~~7~~

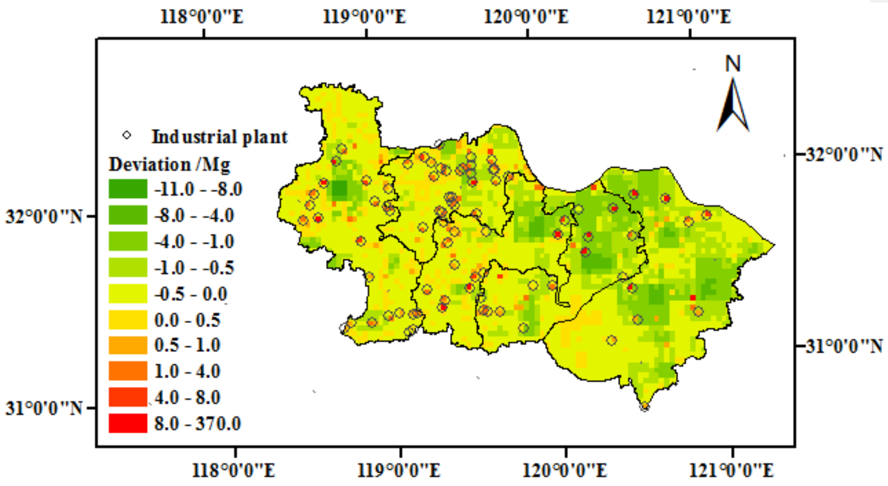
118°0'0"E
119°0'0"E
120°0'0"E
121°0'0"E
N
Industrial plant
Deviation /Mg
-11.0 - -8.0
-8.0 - -4.0
-4.0 - -1.0
-1.0 - -0.5
-0.5 - 0.0
0.0 - 0.5
0.5 - 1.0
1.0 - 4.0
4.0 - 8.0
8.0 - 370.0
32°0'0"N
31°0'0"N

(a)

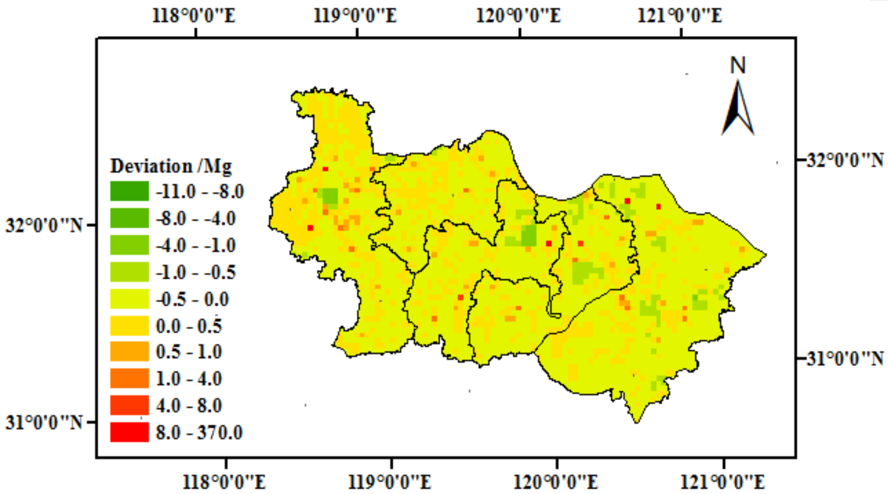
118°0'0"E
119°0'0"E
120°0'0"E
121°0'0"E
N
Deviation /Mg
-11.0 - -8.0
-8.0 - -4.0
-4.0 - -1.0
-1.0 - -0.5
-0.5 - 0.0
0.0 - 0.5
0.5 - 1.0
1.0 - 4.0
4.0 - 8.0
8.0 - 370.0
32°0'0"N
31°0'0"N

(b)

Figure 7~~8~~

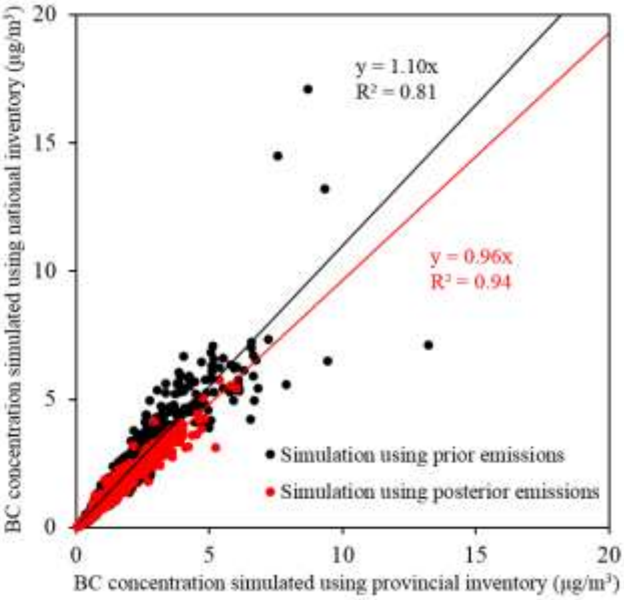
BC concentration simulated using national inventory (μg/m³)
BC concentration simulated using provincial inventory (μg/m³)
0
5
10
15
20
y = 1.10x
R² = 0.81
y = 0.96x
R² = 0.94
Simulation using prior emissions
Simulation using posterior emissions

(a)

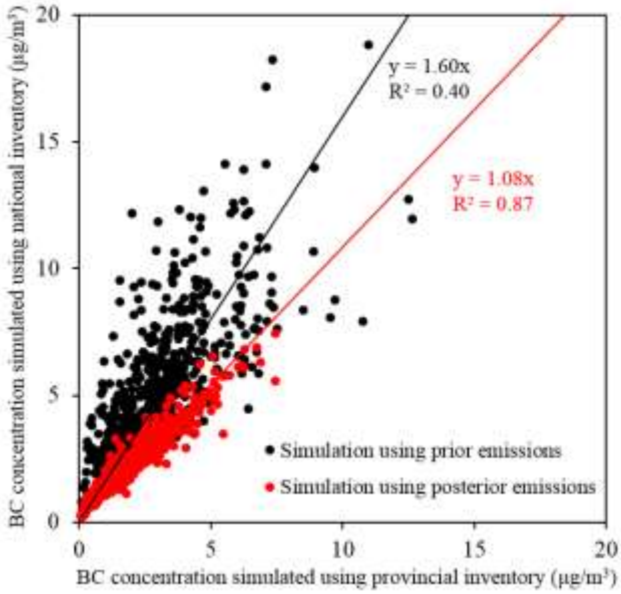
BC concentration simulated using national inventory (μg/m³)
BC concentration simulated using provincial inventory (μg/m³)
0
5
10
15
20
y = 1.60x
R² = 0.40
y = 1.08x
R² = 0.87
Simulation using prior emissions
Simulation using posterior emissions

(b)

~~Figure 9~~

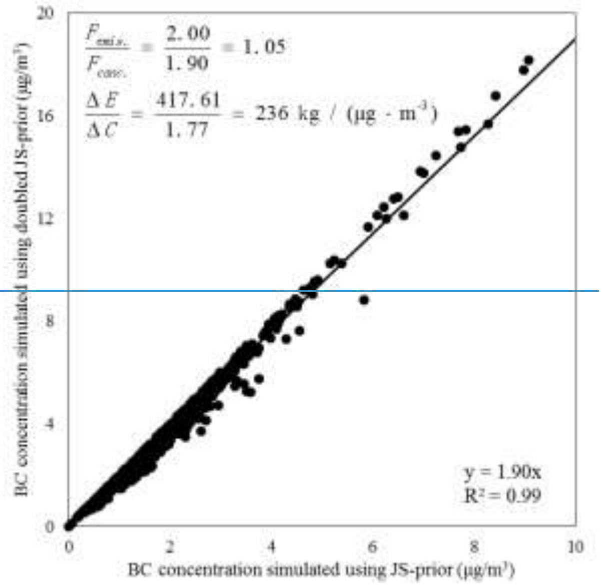

~~(a)~~

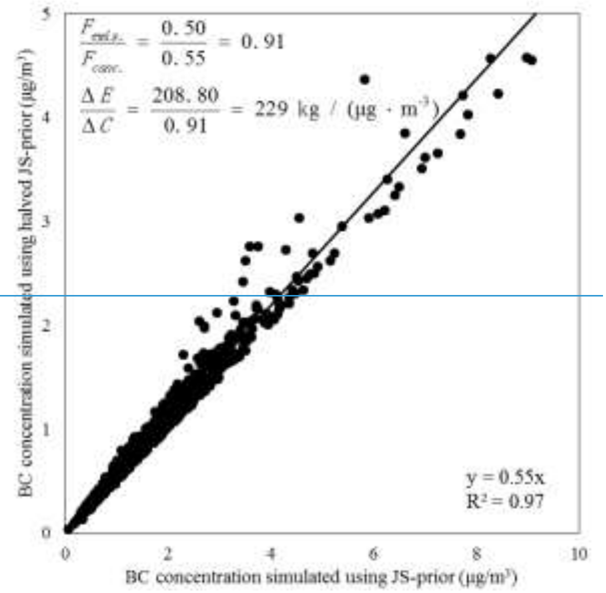

~~(b)~~

带格式的：正文

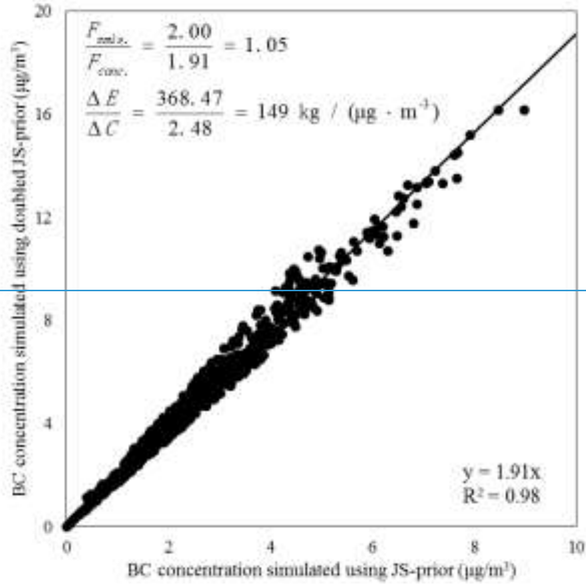
$\frac{F_{emis.}}{F_{conc.}} = \frac{2.00}{1.91} = 1.05$
$\frac{\Delta E}{\Delta C} = \frac{368.47}{2.48} = 149$ kg / (μg · m^{-3})
y = 1.91x
R² = 0.98
BC concentration simulated using doubled JS-prior (μg/m³)
BC concentration simulated using JS-prior (μg/m³)

~~(c)~~

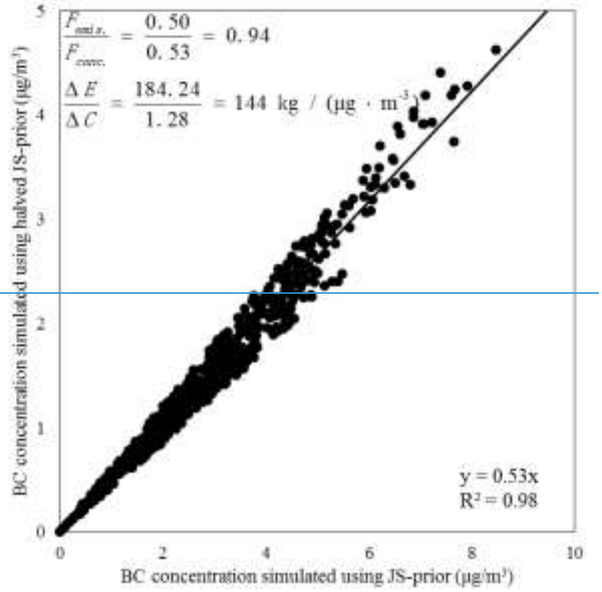
$\frac{F_{emis.}}{F_{conc.}} = \frac{0.50}{0.53} = 0.94$
$\frac{\Delta E}{\Delta C} = \frac{184.24}{1.28} = 144$ kg / (μg · m^{-3})
y = 0.53x
R² = 0.98
BC concentration simulated using halved JS-prior (μg/m³)
BC concentration simulated using JS-prior (μg/m³)

~~(d)~~

带格式的: 正文

~~Figure 10~~

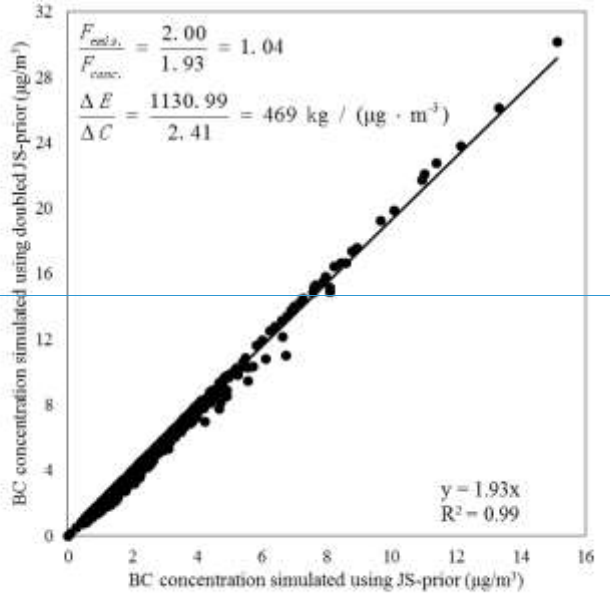

$\frac{F_{emis.}}{F_{conc.}} = \frac{2.00}{1.93} = 1.04$
$\frac{\Delta E}{\Delta C} = \frac{1130.99}{2.41} = 469$ kg / (μg · m^{-3})
y = 1.93x
R² = 0.99
BC concentration simulated using doubled JS-prior (μg/m³)
BC concentration simulated using JS-prior (μg/m³)

~~(a)~~

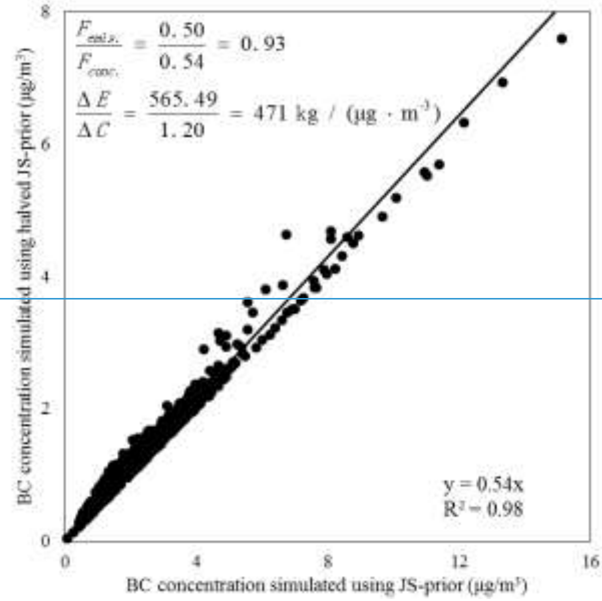

$\frac{F_{emis.}}{F_{conc.}} = \frac{0.50}{0.54} = 0.93$
$\frac{\Delta E}{\Delta C} = \frac{565.49}{1.20} = 471$ kg / (μg · m^{-3})
y = 0.54x
R² = 0.98
BC concentration simulated using halved JS-prior (μg/m³)
BC concentration simulated using JS-prior (μg/m³)

~~(b)~~

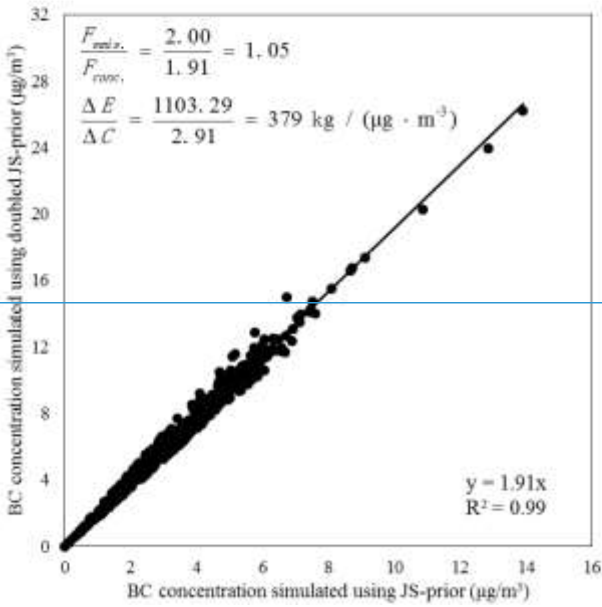

$\frac{F_{emis.}}{F_{conc.}} = \frac{2.00}{1.91} = 1.05$
$\frac{\Delta E}{\Delta C} = \frac{1103.29}{2.91} = 379$ kg / (μg · m^{-3})
y = 1.91x
R² = 0.99
BC concentration simulated using doubled JS-prior (μg/m³)
BC concentration simulated using JS-prior (μg/m³)

~~(c)~~

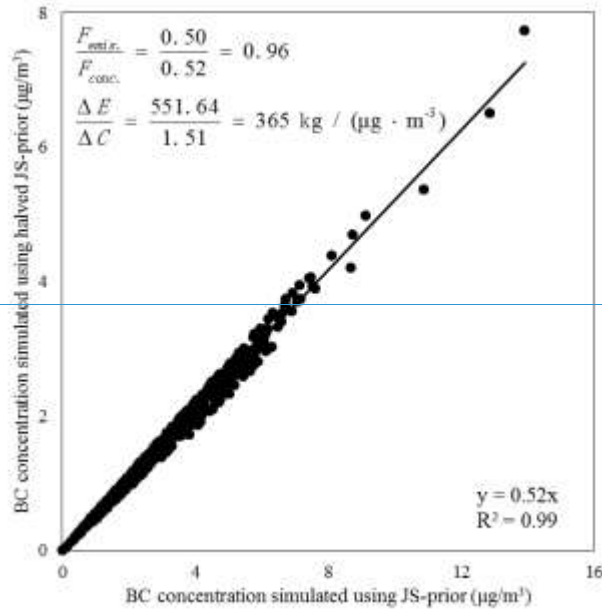

$\frac{F_{emis.}}{F_{conc.}} = \frac{0.50}{0.52} = 0.96$
$\frac{\Delta E}{\Delta C} = \frac{551.64}{1.51} = 365$ kg / (μg · m^{-3})
y = 0.52x
R² = 0.99
BC concentration simulated using halved JS-prior (μg/m³)
BC concentration simulated using JS-prior (μg/m³)

~~(d)~~

Figure 8~~11~~

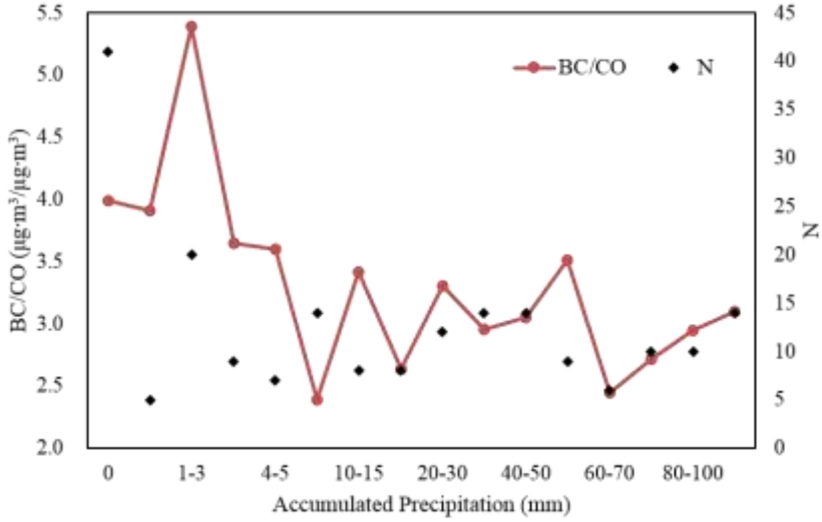

(a)

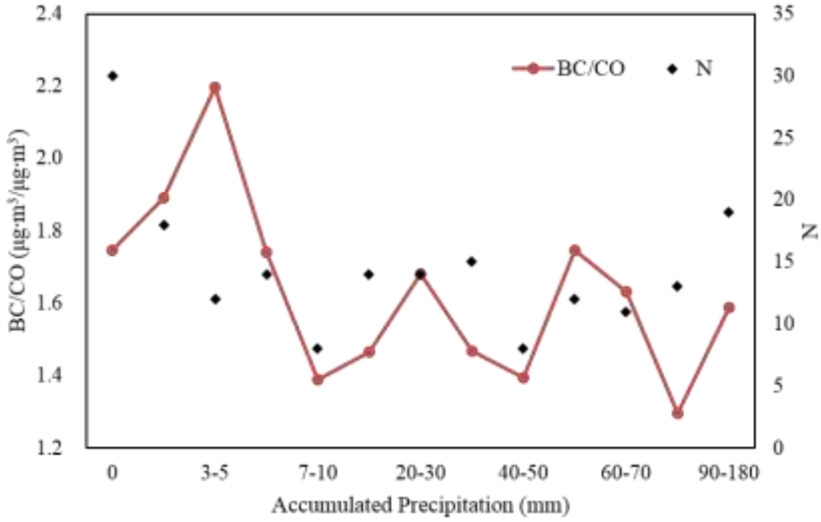

(b)

Figure 9~~12~~

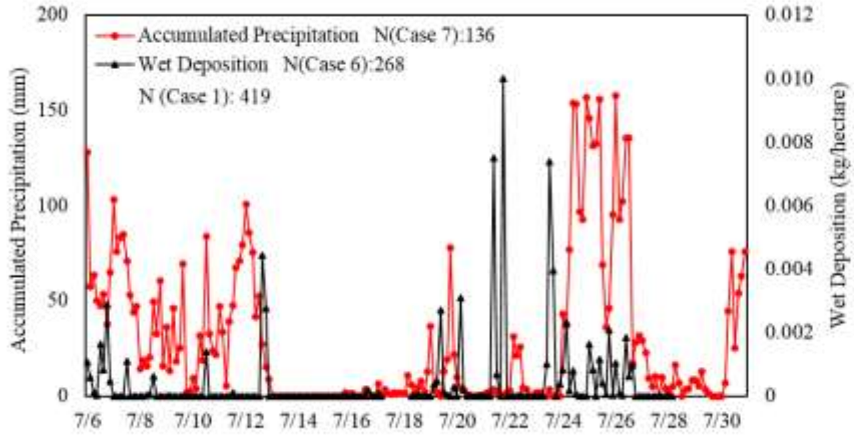

(a)

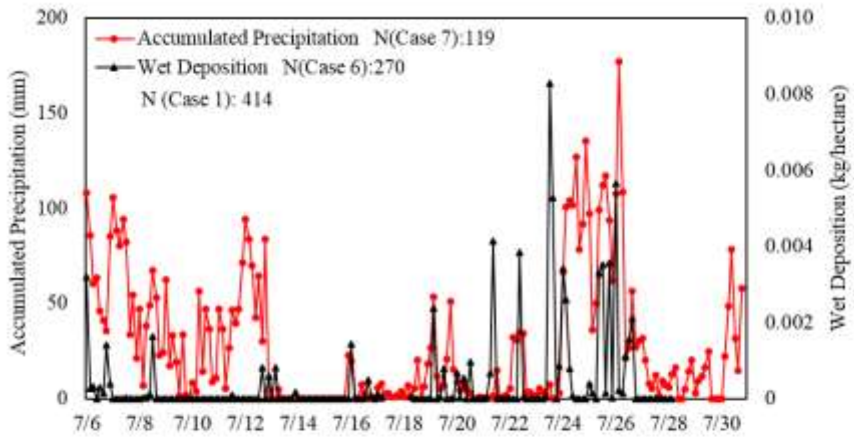

(b)